A study of the properties, reactivity and anticancer activity of novel Nmethylated-3-thiazolyl or 3-thienyl carbazoles and their Pd(II) and Pt(II) complexes

Marta Reig[a], Ramón Bosque[b], Mercè Font-Bardía[c], Carme Calvis[d], Ramon Messeguer[d],
Laura Baldomà[e,f], Josefa Badía[e,f], Dolores Velasco[a], Concepción López[b,*]

a Grup de Materials Orgànics, Institut de Nanociència i Nanotecnologia (IN2UB), Secció de Química Orgànica, Departament de Química Inorgànica i Orgànica, Facultat de Química, Martí i Franquès 1-11, E-08028 Barcelona, Spain
b Secció de Química Inorgànica, Departament de Química Inorgànica i Orgànica, Facultat de Química, Martí i Franquès 1-11, E-08028 Barcelona, Spain
c Unitat de Difracció de Raigs-X, Centres Científics i Tecnològics (CCiT), Universitat de Barcelona, Solé i Sabaris 1–3, E-08028 Barcelona, Spain
d Biomed Division, Health & Biomedicine Unit, LEITAT Technological Center, Parc Científic de Barcelona, Edifici Hèlix, Baldiri i Reixach 13-21, E-08028 Barcelona, Spain
e Secció de Bioquímica i Biología Molecular, Departament de Bioquímica i Fisiologia, Facultat de Farmàcia i Ciències de l'Alimentació, Universitat de Barcelona, Av. Joan XXIII 27-31, E-08028 Barcelona, Spain
f Institut de Biomedicina de la Universitat de Barcelona - Institut Recerca Sant Joan de Deu, Barcelona, Spain

conchi.lopez@qi.ub.es (C. López).

ABSTRACT:

The synthesis and characterization of two hybrid N-methylated carbazole derivatives containing a thiazolyl or a thienyl ring is reported. The thiazolyl derivative has been also characterised by X-ray diffraction analysis. The study of its reactivity in front of [MCl2(dmso)2] (M=Pd or Pt) or Na2[PdCl4] in methanol has allowed us to isolate and characterize its complexes. However, for the thienyl analogue, the formation of any Pd(II) or Pt(II) complex was not detected, indicating that it is less prone to bind to the M(II) ions than its thiazolyl analogue. Density Functional Theory (DFT) and Time-Dependent Density Functional Theory (TD-DFT) calculations have also been carried out in order to rationalize the influence of the nature of the thiazolyl or thienyl group on the electronic delocalization. Molecular mechanics calculations show that the free rotation of the thiazolyl in relation to the carbazole requires a greater energy income than for its thienyl analogue. Studies of the cytotoxic activity of the new compounds on colon (HCT116) and breast (MDA-MB231 and MCF7) cancer cell lines show that the thiazolyl carbazole ligand and its Pt(II) complex are the most active agents of the series and in the MCF7 line their potency is higher than that of cisplatin. In the non-tumoral human skin fibroblast BJ cell line, all the compounds were less toxic than cisplatin. Their potential ability to modify the electrophoretic mobility of pBluescript SK+ plasmid DNA and to act as inhibitors of Topoisomerases I and IIα or cathepsin B has also been investigated.

1. INTRODUCTION

Cancer is among the leading causes of morbidity and death that unfortunately affects millions of persons worldwide (i.e. more than one million each year in USA [1]). The American Cancer Society estimates an incidence of ca. 1.7 million new cases for 2017 and>0.6 million deaths [2] mainly produced by colorectal, breast, lung and ovarian cancers [2–4]). Every cancer type needs a specific treatment protocol that usually involves chemotherapy (CT) [5], radiotherapy and/or surgery. The development of new antitumor drugs with improved activities and lower side effects than those used nowadays in CT is still one of the main challenges of current research in medicinal chemistry. Among the variety of strategies used nowadays in drug discovery [6–11], those with greater expectations are based on: a) natural products and/or b) new synthetic products with several bioactive arrays (i.e. by incorporation of an additional bioactive unit in the backbones of commercially available pharmaceuticals or known drugs and commonly known as "molecular hybridization approach") [6–11].

On the other hand, it is well-known that heterocycles and their derivatives are one of the most important types of organic compounds due to their outstanding physical and photo-optical properties, their rich reactivity, their utility as ligands in Coordination and Organometallic Chemistry and their multiple applications in a variety of fields, including medicinal chemistry [12–21]. Heterocyclic cores are present in huge range of natural and marketed antimicrobial, anti-inflammatory, antiviral, anticancer, antihypertensive, antimalarial, anti-HIV, antidepressant, antihelmintic drugs, among others. Their relevance in new drugs design and development is undeniable [12–14]. For instance, among all the anticancer drugs approved by FDA during the late five years ca. 75% have heterocyclic arrays with N and/or S atoms or polycyclic aromatic compounds with heterocyclic fragments [15–22].

Carbazole (Fig. 1), thiazole and thiophene are probably three of the most important scaffolds in drug design and discovery [23–33]. These units are present in diverse bioactive synthetic -and even in naturally occurring products. For instance, Ellipticine and Glybomine-C (Fig. 1) isolated from plants, are potent cytotoxic agents in several cancer cell lines [34,35] and the discovery that N-alkylation of Ellipticine enhanced inhibition growth activity has stimulated the interest on N-substituted carbazoles [23–26,34,35]. The number of potent cytotoxic (substituted and/or anellated) carbazoles reported in the last 2 years has grown exponentially and according to a recent review published by Caruso et al. [26]: "Carbazoles are promising scenarios for breast cancer treatments".

In addition to carbazoles, and in a lesser extent, thiazole and thiophene derivatives are gaining increasing interest as "central cores" or as "pendant" groups in drug engineering and specially as promising platforms or "templates" to build up new and more efficient antitumor agents that could overcome or at least reduce the main problems (i.e. drug resistance, toxicity, or other undesirable side effects) associated to drugs used currently. cis-[PtCl2(NH3)2] (cisplatin) and doxorubicin [4,36–40] are two CT agents used in cancer treatments that may generate severe-side effects (i.e. nephrotoxicity, neurotoxicity, the increase of blood pressure, severe nausea, vomiting, or diarrhoea produced by

108 cisplatin or severe heart problems (cardiomyopathy) associated to doxorubicin [36–40]). Since the

109 discovery of cisplatin, the development of metal coordination complexes as anticancer agents has

110 attracted a great deal of interest to obtain more effective and less toxic drugs [41]. For instance, trans-

111 platinum(II) based complexes or those based on less toxic metals (ruthenium, gold or copper) are shown

112 to be promising candidates in safer cancer therapy.

113 Despite of the interest in electronics and materials science arisen by hybrid carbazole/thienyl derivatives

114 [42–52] and the potential synergic effect of the presence of two bioactive arrays [i.e. the N-substituted

115 carbazole and a thiazole (or a thienyl) unit] in the same molecule that could be relevant in drug design

116 [53,54] and in photodynamic therapy (PTD) [55], studies on their biological activities are scarce.

117 Moreover, it is well-known that heterocycles are valuable ligands in Coordination and Organometallic

118 Chemistry [15–17] and their binding to a transition metal ion (Mm+) commonly affects their properties

119 and their biological and/or catalytic activities. For instance, Pd(II) and Pt(II) complexes with

120 heterocyclic ligands (i.e. pyrazoles, indoles) showing greater cytotoxic activity than the free ligands

121 have been reported [56–60]. However, parallel studies on hybrid carbazole/thiazole or thiophene

122 derivatives have not been investigated yet. Therefore, there is a lack of information on their coordination

123 ability and the effect produced by the binding of these ions on their properties and especially on their

124 cytotoxic activity.

125 In this paper, we present two new carbazole derivatives: 9-methyl-3- (2-thiazolyl)-9H-carbazole (1a)

126 and 9-methyl-3-(2-thienyl)-9H-carbazole (1b) shown in Scheme 1, a study of their reactivity in front of

127 Pd (II) and Pt(II), their spectroscopic properties and the anticancer activity of the free ligands and the

128 new Pd(II) and Pt(II) complexes, trans- [PdCl2(1a)2] (2a) and trans-[PtCl2(1a)dmso] (3a).

129

2. EXPERIMENTAL

2.1. Chemistry

2.1.1. Materials and methods

[MCl2(dmso)2] {trans- for M=Pd or cis- for M=Pt} and 3-iodo-9H-carbazole were prepared as described previously [61–63], and the remaining reagents were obtained from commercial sources and used as received. The success of the synthesis of the Pt(II) compound 3a is strongly dependent on the quality of the methanol; the presence of water produces the formation of metallic platinum, other undesirable minor by-products and a significant decrease in the yield. Thus, the use of high quality MeOH (HPLC grade) is required. The remaining solvents used were dried and distilled before use [64]. During the preparation of the complexes (2a and 3a), the reaction flask was protected from the light with aluminium foil. Elemental analysis were carried out at the Centres Científics i Tecnològics (CCiT, Univ. Barcelona) with an Eager 1108 microanalyzer. Mass spectra (ESI+) were performed at the Servei d'Espectrometria de Masses (Univ. de Barcelona) using a LC/MSD-TOF Agilent Technologies instrument. UV–vis. spectra of CH2Cl2 solutions of the free ligands (1a and 1b) and complexes 2a and 3a were recorded at 298 K with a Varian Cary UV–Vis-NIR 500E spectrometer and their emission spectra were obtained on a PTI fluorimeter equipped with a 220B lamp power supply, a 815 photomultiplier detection system and Felix 32 software at 298 K in CH2Cl2 solutions. 1,4-Bis(5-phenyl-2-oxazolyl) benzene (POPOP) dissolved in cyclohexane was used as a standard for the fluorescence quantum yield determination (λexc=300 nm, ΦPOPOP=0.93). 1H and 13C{1H}-NMR spectra were recorded at 298 K in acetone-d6 for the precursor (3-iodo-9-methyl-9H-carbazole) or in CDCl3 (in the remaining cases) with a Varian Mercury 400 MHz or a Bruker 400 MHz Avance III [for 1H and 13C{1H}] and a Bruker 250 MHz and a Bruker 400 Avance III HD (for 195Pt{1H}) spectrometers. Chemical shifts are given in δ values (ppm) using the solvent peaks as internal references (1H and 13C) and H2PtCl6 in D2O (195Pt{1H}) and coupling constants (J) are given in Hz. Abbreviations used for the multiplicities are as follows: s (singlet), d (doublet), dd (doublet of doublets), t (triplet), q (quadruplet) and m (multiplet). The atom numbering system used in the assignment of 1H and 13C{1H}-NMR data is shown in Fig. 2.

2.1.2. Synthesis of ligands 1a and 1b

2.1.2.1. Synthesis of the precursor 3-iodo-9-methyl-9H-carbazole. NaH (240 mg, 6.00 mmol, 60% dispersion in mineral oil) was added to a solution of 3-iodo-9H-carbazole (1.60 g, 5.46 mmol) in anhydrous DMF (10 mL) under nitrogen atmosphere. The solution was stirred at room temperature for 30 min. Then, iodomethane (374 μL, 6.00 mmol) was added and the mixture was stirred at room temperature for 30 min and then treated with water. The aqueous layer was extracted with CH2Cl2 and

the organic layer was dried over Na2SO4, filtered off and the solvent was distilled off under reduced pressure. The crude was purified by flash column chromatography using a mixture of hexane and ethyl acetate (20:1 v/v) as the eluent to give 3-iodo-9-methyl-9H-carbazole (1.45 g, 86%). 1H NMR (400 MHz, acetone-d6) δ (ppm): 8.49 (d, 4JHH= 1.7, 1H, H4), 8.17 (d, 3JH-H=7.6, 1H, H5), 7.74 (dd, 3JH-H=8.6, 4JH-H=1.7, 1H, H2), 7.55 (d, 3JH-H=8.2, 1H, H8), 7.53–7.48 (m, 1H, H7), 7.42 (d, 3JH-H=8.6, 1H, H1), 7.26–7.22 (m, 1H, H6), 3.91 (s, NMe, 3H). CI-MS (m/z): calc. For C13H11IN (M+H)+ 308.0, found: 308.0.

2.1.2.2. Synthesis of 9-methyl-3-(2-thiazolyl)-9H-carbazole (1a). A mixture of 3-iodo-9-methyl-9H-carbazole (1.24 g, 4.04 mmol), 2- (tributylstannyl)thiazole (1.81 g, 4.84 mmol) and Pd(PPh3)4 (231 mg, 0.20 mmol) in anhydrous DMF (10 mL) was heated to 100 °C under a nitrogen atmosphere for 20 h. Then, the reaction mixture was cooled down to room temperature, treated with water and the product was extracted with dichloromethane. The organic layer was dried over Na2SO4, filtered off and the solvent was distilled off under reduced pressure. The crude was purified by flash column chromatography using a mixture of hexane and CH2Cl2 (5:1 v/v) as the eluent to give compound 1a (420 mg, 39%). 1H NMR (400 MHz, CDCl3) δ (ppm): 8.73 (d, 4JH-H=1.7, 1H, H4), 8.16 (d, 3JH-H=8.0, 1H, H5), 8.10 (dd, 3JHH= 8.6, 4JH-H=1.7, 1H, H2), 7.87 (d, 3JH-H=3.3, 1H, H4'), 7.54–7.50 (m, 1H, H7), 7.44 (d, 3JH-H=8.6, 1H, H1), 7.43 (d, 3JH-H=8.2, 1H, H8), 7.31–7.27 (m, 2H, H6 and H5'), 3.89 (s, 3H, NMe). 13C NMR (100 MHz, CDCl3) δ (ppm): 170.0 (C2'), 143.4 (C4'), 142.2 (C9a), 141.7 (C8a), 126.5 (C7), 125.1 (C3), 124.9 (C2), 123.3 (C4a), 123.0 (C5a), 120.8 (C5), 119.7 (C6), 119.0 (C4), 117.8 (C5'), 108.9 (2C, C1 and C8), 29.4 (NCH3). HRMS (ESI-MS) (m/z): calc. for C16H13N2S (M+H)+: 265.0794, found: 265.0796. Elemental Anal. (%). Calc. for C16H12N2S (MW=264.34). C, 72.70; H, 4.58; N, 10.60 and S, 12.13; found: C, 72.65; H, 4.65; N, 10.53; and S, 11.86.

2.1.2.3. Synthesis of 9-methyl-3-(2-thienyl)-9H-carbazole (1b). A mixture of 3-iodo-9-methyl-9H-carbazole (771 mg, 2.51 mmol), 2-(tributylstannyl)thiophene (1.12 g, 3.00 mmol) and Pd(PPh3)4 (139 mg, 0.12 mmol) in anhydrous DMF (10 mL) was heated to 100 °C under a nitrogen atmosphere for 24 h. Then, the reaction mixture was cooled down to room temperature, treated with water and the product was extracted with dichloromethane. The organic layer was dried over Na2SO4, filtered off and the solvent was distilled off under reduced pressure. The crude was purified by flash column chromatography using a mixture of hexane and dichloromethane (9:1 v/v) as the eluent to give compound 1b (343 mg, 52%). 1H NMR (400 MHz, CDCl3) δ (ppm): 8.32 (d, 4JH-H=1.8, 1H, H4), 8.14 (d, 3JH-H=7.7, 1H, H5), 7.75 (dd, 3JH-H=8.5, 4JH-H=1.8, 1H, H2), 7.52–7.48 (m, 1H, H7), 7.41 (d, 3JH-H=8.1, 1H, H8), 7.40 (d, 3JH-H=8.5 Hz, 1H, H1), 7.35 (dd, 3JHH= 3.6, 4JH-H=1.0, 1H, H3'), 7.28–7.24 (m, 2H, H5' and H6), 7.11 (dd, 3JH-H=5.1, 3JH-H=3.6, 1H, H4'), 3.87 (s, 3H, NMe). 13C NMR (100 MHz, CDCl3) δ (ppm): 146.0 (C2'), 141.6 (C8a), 140.7 (C9a), 128.1 (C4'), 126.2 (C7),

125.9 (C3), 124.5 (C2), 123.8 (C5'), 123.3 (C4a), 122.9 (C5a), 122.2 (C3'), 120.6 (C5), 119.3 (C6), 118.0 (C4), 108.9 (C1 or C8), 108.8 (C1 or C8), 29.4 (NMe). HRMS (ESI-MS) (m/z): calc. for $C_{17}H_{14}NS$ (M+H)+ 264.0841, found: 264.0843; elemental Anal (%). Calc. for $C_{17}H_{13}NS$ (MW=263.34). C, 77.53; H, 4.98; N, 5.32 and S, 12.70; found: C, 77.45; H, 5.04; N, 5.25; and S, 12.61.

2.1.3. Preparation of the complexes 2a and 3a

2.1.3.1. Synthesis of compound 2a. This compound was obtained using two alternative procedures that differ in the nature of the starting Pd(II) complex used as reagent: trans-[PdCl2(dmso)2] or Na2[PdCl4] {methods a) and b), respectively}. Method b) allows the isolation of compound 2a with a higher yield (and at lower temperatures) than using method a). Method a) trans-[PdCl2(dmso)2] (63 mg, 0.19 mmol) was treated with 30 mL of methanol, refluxed until complete dissolution and filtered out. Then, 50 mg (0.19 mmol) of carbazole 1a, were added to the hot filtrate and the mixture was refluxed for 1 h. After this period, the resulting solution was allowed to cool down to room temperature and the solid formed was collected by filtration, air-dried and later on dried in vacuum for 2 days. (Yield: 38 mg, 28%). Method b) A solution containing Na2[PdCl4] (28 mg, 0.095 mmol) and 20 mL of methanol was added to another one formed by ligand 1a (50 mg, 0.19 mmol) and 5 mL of methanol. The resulting mixture was stirred for 24 h at 298 K. After this period, the solid formed was collected by filtration and dried as in Method a) (Yield: 55 mg, 82%). 1H NMR (400 MHz, CDCl3) δ (ppm): 9.22 (d, 4JH-H=1.8, 2H, 2H4), 8.47 (dd, 3JH-H=8.5, 4JH-H=1.8, 2H, 2H2), 8.19 (d, 3JH-H=7.7, 2H, 2H5), 8.08 (d, 3JH-H=3.7, 2H, 2H4'), 7.58–7.44 (m, 8H, 2H1, 2H7, 2H8 and 2H5'), 7.32 (t, 3JH-H=7.7, 2H, 2H6), 3.93 (s, 6H, 2NMe). Elemental Anal. (%). Calc. for $C_{32}H_{24}Cl_2N_4PdS_2$ (MW=706.01). C, 54.44; H, 3.43; N, 7.94 and S, 9.08; found: C, 54.50; H, 3.50; N, 8.03 and S, 8.85.

2.1.3.2. Synthesis of compound 3a. cis-[PtCl2(dmso)2] (80 mg, 0.19 mmol) was suspended in 30 mL of methanol, until complete dissolution. Then, the hot solution was filtered out and the filtrate was poured into a methanol solution (5 mL) of ligand 1a (50 mg, 0.19 mmol). The reaction flask was protected from light with aluminium foil and the mixture was refluxed for 1 h and filtered. Then, the filtrate was afterwards concentrated to dryness on a rotary evaporator and the residue was dried in vacuum for 24 h. After this period, the solid was dissolved in the minimum amount of CH2Cl2 (ca. 15 mL) and passed through a short SiO2 column (5.0 cm×1.5 cm). Elution with CH2Cl2 released a pale yellowish band that was collected and concentrated to dryness on a rotary evaporator giving 3a (yield: 69 mg, 60%). 195Pt{1H}-NMR data (54 MHz, CDCl3) δ (ppm): −2983 (s). 1H NMR-data (400 MHz, CDCl3) δ (ppm): 9.22 (d, 4JH-H=1.8, 1H, H4), 8.47 (dd, 3JH-H=8.5, 4JH-H=1.8, 1H, H2), 8.20 (d, 3JH-H=7.7, 1H, H5), 8.08 (d, 3JH-H=3.7, 1H, H4'), 7.58–7.54 (m, 2H, H1 and H7), 7.47 (d, 3JH-H=8.2, 1H, H8), 7.46 (d, 3JH-H=3.7, 1H, H5'), 7.34–7.30 (m, 1H, H6), 3.94 (s, 3H, NMe), 3.37 (s, 6H, dmso). ESI-MS (m/z): calc. for $C_{18}H_{19}Cl_2N_2OPtS_2$ (M+H)+ 608.0, found: 608.0. Elemental Anal. (%). Calc. for:

240 C18H18Cl2N2OPtS2 (MW=608.46): C, 35.53; H, 2.98; N, 4.60 and S, 10.54; found C, 35.59; H, 3.05;
241 N, 4.63 and S, 10.60.

242

243 2.1.3.3. Synthesis of the two isomers of [PtCl2(1a)(dmso)] {trans-(3a) and cis-(4a)}. NaAcO (16 mg,
244 0.19 mmol) was dissolved in 5 mL of methanol at 298 K and then added dropwise to a mixture formed
245 by carbazole 1a (50 mg, 0.19 mmol), cis-[PtCl2(dmso)2] (80 mg, 0.19 mmol) and 25 mL of toluene. The
246 flask was protected from the light with aluminium foil and refluxed for 3 days. After this period the deep
247 brown solution was filtered through a Celite pad, and the filtrate was concentrated on a rotary
248 evaporator. The dark residue was dried in vacuum for 24 h, dissolved in CH2Cl2 (ca. 30 mL) and finally
249 passed through a short (5.0 cm×1.5 cm) SiO2 column. Elution with CH2Cl2 released a wide pale yellow
250 band that was collected in portions (ca. 25 mL/each). The first collected fractions ca. 120 mL gave after
251 concentration 11 mg of 3a; while the remaining subsequent fractions eluted (ca. 200 mL) gave, after
252 concentration a solid (26 mg) containing isomers 3a and 4a (in a ca. equimolar ratio. %). 195Pt{1H}-
253 NMR data (54 MHz, CDCl3, see also Fig. S1, A) δ (ppm): −2980 (s) (trans-isomer, 3a) and−2932 (s)
254 (cis-isomer, 4a); 1H NMR data (400 MHz, CDCl3) δ (ppm): (see also Fig. S1, B): 9.22 (d, 4JH-H=1.8,
255 1H, H4 of 3a), 8.47 (dd, 3JH-H=8.5, 4JH-H=1.8, 1H, H2 of 3a), 8.20 (d, 3JH-H=7.7, 1H, H5 of 3a),
256 8.08 (d, 3JH-H=3.7, 1H, H4' of 3a), 7.58–7.54 (m, 2H, H1 and H7 of 3a), 7.47 (d, 3JH-H=8.2, 1H, H8
257 of 3a), 7.46 (d, 3JH-H=3.7, 1H, H5'), 7.34–7.30 (m, 1H, H6 of 3a), 3.98 (s, 3H, NMe of 4a); 3.94 (s,
258 3H, NMe of 3a), 3.37 (s, 6H, Me(dmso) of 3a); 3.25 [s, 3H, Me(dmso) of 4a]; and 2.29 [s, 3H,
259 Me(dmso) of 4a]. ESI-MS (m/z): calc. for C18H19Cl2N2OPtS2 (M+H)+=608.0; found: 608.0.
260 Elemental Anal. (%). Calc. for: C18H18Cl2N2OPtS2 (MW=608.46): C, 35.53; H, 2.98; N, 4.60 and S,
261 10.54; found C, 35.59; H, 3.15; N, 4.54 and S, 10.37.

262

263 2.2. Crystallography
264 A colourless prism-like specimen of C16H12N2S (1a) (sizes in Table 1) was used for the X-ray
265 crystallographic analysis. The X-ray intensity data were measured on a D8 Venture system equipped
266 with a multilayer monochromator and a Mo microfocus (λ=0.71073 Å). The frames were integrated with
267 the Bruker SAINT software package using a narrow-frame algorithm. The integration of the data using
268 an orthorhombic unit cell yielded a total of 7259 reflections to a maximum θ angle of 27.50° (0.77 Å
269 resolution), of which 2855 were independent (average redundancy 2.543, completeness=99.9%,
270 Rint=3.42%, Rsig=4.25%) and 2482 (86.94%) were greater than 2σ(F2). The final cell constants given
271 in Table 1 are based upon the refinement of the XYZ-centroids of reflections above 20 σ(I). The
272 calculated minimum and maximum transmission coefficients (based on crystal size) are 0.6711 and
273 0.7456. The structure was solved using the Bruker SHELXTL Software Package, and refined using
274 SHELXL [65], using the space group P212121, with Z=4 for the formula unit, C16H12N2S. The final
275 anisotropic full-matrix least-squares refinement on F2 with 173 variables converged at R1=3.58%, for
276 the observed data and wR2=8.01% for all data. The goodness-of-fit was 1.074. The largest peak in the

277 final difference electron density synthesis was 0.241 e-/Å3 and the largest hole was −0.234 e-/Å3 with

278 an RMS deviation of 0.053 e-/Å3. Further details concerning the resolution and refinement of the crystal

279 structure are presented in Table 1. CCDC-1560144 contains the crystallographic data of this paper.

280 These data can be obtained from the Cambridge Crystallographic Data Centre via:

281 www.ccdc.cam.ac.uk/data. request.cif.

282

283 2.3. Computational details

284 The conformational map has been searched at the molecular mechanics level using the augmented

285 MMFF94 method [66] as implemented in Spartan [67]. The dihedral angle S1-C2-C3-C4 (φ) has been

286 sampled every 5° and the remaining geometric parameters have been fully optimized. DFT [68]

287 calculations have been performed using the B3LYP functional [69,70] implemented in the Gaussian 03

288 software [71] and the 6-31G* basis set [72,73], including polarization functions for the non-hydrogen

289 atoms.

290

291 2.4. Biological studies

292 2.4.1. Cell culture

293 Colon adenocarcinoma (HCT116) cells (from the American Type Culture Collection) and breast cancer

294 (MDA-MB231 and MCF7) cells (from European Collection of Cell Cultures, ECACC) were used for all

295 the experiments. Cells were grown as a monolayer culture in DMEM-high glucose (Sigma, D5796) in

296 the presence of 10% heat-inactivated fetal calf serum and 0.1% streptomycin/penicillin in standard

297 culture conditions.

298 The human skin fibroblast cell line BJ was cultured in MEM (Sigma, M2279) in the presence of 10%

299 FBS, 4mM glutamine, and 0.5% streptomycin/penicillin. All the cells were incubated under standard

300 conditions (humidified air with 5% CO2 at 37 °C). The cells were passaged at 90% confluence by

301 washing once with cation-free HBSS followed by a 3 min incubation with trypsin ([0.5 µg/mL]/EDTA

302 [0.2 µg/ mL]) (Gibco-BRL, 15400054) solution in HBSS at 37 °C, and transferred to its medium. Prior

303 to seeding at a defined cell concentration, the cells were recovered from the medium by centrifugation

304 and counted.

305

306 2.4.2. Cell viability assays

307 For these studies, compounds were dissolved in 100% DMSO at 50mM as stock solution; then,

308 consecutive dilutions have been done in DMSO (1:1) (in this way DMSO concentration in cell media

309 was always the same); followed by 1:500 dilutions of the solutions of compounds on cell media. The

310 assay was carried out as described by Givens et al. [74]. In brief, MDA-MB231 and MCF7 cells were

311 plated at 5000 cells/well or 10,000 cells/well respectively, in 100 µL media in tissue culture 96 well

312 plates (Cultek). BJ cells were plated at 2500 cells per well. After 24 h, medium was replaced by 100

313 µL/well of serial dilution of drugs. Each point concentration was run in triplicate. Reagent blanks,

containing media plus colorimetric reagent without cells were run on each plate. Blank values were subtracted from test values and were routinely 5–10% of uninhibited control values. Plates were incubated for 72 h. Hexosamidase activity was measured according to the following protocol: the media containing the cells was removed and cells were washed once with phosphate buffer saline (PBS) 60μL of substrate solution (p-nitrophenol-N-acetyl-β-D-glucosamide 7.5mM [Sigma N-9376], sodium citrate 0.1 M, pH=5.0, 0.25% Triton X-100) was added to each well and incubated at 37 °C for 1–2 h; after this incubation time, a bright yellow colour appeared; then, plates could be developed by adding 90 μL of developer solution (Glycine 50 mM, pH=10.4; EDTA 5 mM), and absorbance was recorded at 410 nm.

2.4.3. DNA migration studies

A stock solution (10 mM) of each compound was prepared in high purity DMSO. Then, serial dilutions were made in MilliQ water (1:1). Plasmid pBluescript SK+ (Stratagene) was obtained using a QIAGEN plasmid midi kit as described by the manufacturer. Interaction of drugs with pBluescript SK+ plasmid DNA was analysed by agarose gel electrophoresis following a modification of the method described by Abdullah et al. [75]. Plasmid DNA aliquots (40 μg/mL) were incubated in TE buffer (10mM Tris-HCl, 1mM EDTA, pH 7.5) with different concentrations of compounds 1a, 1b, 2a and 3a ranging from 0 to 200 μM at 37 °C for 24 h. Final DMSO concentration in the reactions was always lower than 1%. For comparison, cisplatin (1–10 μM) and ethidium bromide (EB, 10μM) were used as reference controls. Aliquots of 20 μL of the incubated solutions of compounds containing 0.8 μg of DNA were subjected to 1% agarose gel electrophoresis in TAE buffer (40mM Trisacetate, 2mM EDTA, pH 8.0). The gel was stained in TAE buffer containing ethidium bromide (ET, 0.5 mg/mL) and visualized and photographed under UV light.

2.4.4. DNA topoisomerase I and topoisomerase IIα inhibition assays Topoisomerase I-based

experiments were performed as described previously [76]. Supercoiled pBluescript DNA, obtained as described above, was treated with Topoisomerase I in the absence or presence of increasing concentrations of compounds 1a, 1b, 2a and 3a. Assay mixtures contained supercoiled pBluescript DNA (0.8 μg), calf thymus Topoisomerase I (3 units) and compounds 1a, 1b, 2a or 3a (0–200 μM) in 20 μL of relaxation buffer Tris-HCl buffer (pH 7.5) containing 175mM KCl, 5mM MgCl2 and 0.1mM EDTA. Ethidium bromide (EB, 10 μM) was used as a control of intercalating agents and etoposide (E, 100 μM) as a control of the non-intercalating agent. Reactions were incubated for 30 min at 37 °C and stopped by the addition of 2 μL of agarose gel loading buffer. Samples were then subjected to electrophoresis and DNA bands stained with ethidium bromide as described above.
To distinguish whether compounds act as Topoisomerase inhibitors or DNA intercalators the conversion of relaxed DNA to a supercoiled state caused by the compounds was analysed in the presence of Topoisomerase I. Relaxed DNA was obtained by incubation of supercoiled DNA with Topoisomerase I as described above. Assay mixtures (20 μL) contained: relaxed DNA, Topoisomerase I (3 units) and

351 compound (50 μM or 100 μM). Reactions were incubated 20 min at 37 °C and stopped as described

352 above. Ethidium bromide (10 μM) was used as a control of intercalative drug.

353 The DNA Topoisomerase IIα inhibitory activity of the compounds tested in this study was measured as

354 follows. Supercoiled pBluescript DNA was incubated with Topoisomerase IIα (Affymetrix) in the

355 absence or presence of increasing concentrations of compounds under analysis. Assay mixtures

356 contained supercoiled pBluescript DNA (0.3 μg), Topoisomerase IIα (4 units) and the tested compounds

357 (0–200 μM) in 20 μL of 1× Topo II reaction buffer (PN73592). Etoposide was used as a control of Topo

358 IIα inhibitor. Reactions were incubated for 45 min at 37 °C and stopped by the addition of 2 μL of

359 agarose gel loading buffer. Samples were then subjected to electrophoresis and DNA bands stained with

360 ethidium bromide as described before.

361

362 2.4.5. Cathepsin B inhibition assay

363 The colorimetric cathepsin B assay was performed as described by Casini et al. [77] with few

364 modifications. Briefly, the reaction mixture contained 100mM sodium phosphate (pH 6.0), 1mM EDTA

365 and 200 μM sodium N-carbobenzoxy-L-lysine p-nitrophenyl ester as the substrate.

366 To have the enzyme catalytically active before each experiment the cysteine in the active site was

367 reduced by treatment with dithiothreitol (DTT). For this purpose, 5mM DTT was added to the cathepsin

368 B sample, before dilution, and incubated 1 h at 30 °C. To test the inhibitory effect of the compounds on

369 cathepsin B, activity measurements were performed in triplicate using fixed concentrations of enzyme

370 (500 nM) and substrate (200 μM). The compounds were used at concentrations ranging from 5 to 100

371 μM. Previous to the addition of substrate, cathepsin B was incubated with the different compounds at 25

372 °C for 2 h. The cysteine proteinase inhibitor E-64 was used as a positive control of cathepsin B

373 inhibition. Complete inhibition was achieved at 10 μM concentration of E-64. Activity was measured

374 over 90 s at 326 nm on a UV-spectrophotometer.

375

376

377

378

379

380

381

382

3. RESULTS AND DISCUSSION

3.1. Synthesis and characterization

3.1.1. Synthesis of the ligands

The new carbazole derivatives: 9-methyl-3-(2-thiazolyl)-9H-carbazole (1a) and 9-methyl-3-(2-thienyl)-9H-carbazole (1b) were prepared from commercially available carbazole in a three-step-sequence of reactions (Scheme 1), that involved the iodination of the 9H-carbazole [63] followed by the alkylation to produce the 3-iodo-9-methyl-9Hcarbazole [78], that later on reacted with either 2-(tributylstannyl) thiazole (for 1a) [79,80] or 2-(tributylstannyl)thiophene (for 1b) via Stille coupling reaction [81] to produce the final products. All compounds were entirely characterized by 1H NMR and 13C{1H} NMR spectroscopies, mass spectrometry and elemental analyses.

The crystal structure of compound 1a (Fig. 3) confirmed the presence of the thiazolyl group on position 3. In compound 1a, the nitrogen atom of the thiazolyl unit (N1) is on the same side as the Me group. As a consequence of this arrangement of groups, the N1 atom is proximal to the hydrogen atom H12 of the carbazole unit while the S1 atom is relatively close to the H4 atom. The distances N1···H12 (2.580 Å) and S1···H4 (2.751 Å) are smaller than the sum of the van der Waals radii of the atoms involved (N, 1.55 Å; H, 0.95 Å and S, 1.85 Å) [82–87]. Thus suggesting the existence of non-conventional CeH···N and CeH···S intramolecular hydrogen bonds [88], similar to those found in most 2-phenylthiazole derivatives [82–86,89–92].

The thiazolyl group is planar and slightly twisted (ca. 13.9°) in relation to the main plane of the carbazole array. In the crystal, the relative orientation of the molecules (Fig. 4, A) allows $\pi \cdots \pi$ interactions between the heterocyclic array of a unit at (x, y, z) and the substituted phenyl ring of another one at (1+x, y, z) (the distance between the centroids of these rings is 3.90 Å). In addition, one of the hydrogen atoms of the methyl group is at only 2.77 Å from the centroid of the phenyl ring of a parallel unit, indicating the existence of intermolecular CeH···π contacts. As a consequence of this, the assembly of the molecules results in pillars (Fig. 4, A). These structural units are connected by additional CeH···π short contacts (Fig. 4, B) involving the H3 atom of the heterocyclic units in one of the pillars and the centroids of the thiazolyl groups of another one.

3.1.2. Coordination capability of the new hybrid carbazoles 1a and 1b In view of their potential

biological activities (i.e. anticancer, antibacterial), we decided to evaluate the coordination abilities of the new carbazoles in front of the Pd(II) and Pt(II) ions. In a first stage, we selected ligand 1a and studied its reactivity with [MCl2(dmso)2] {transfor M=Pd or cis- for M=Pt} or Na2[PdCl4] under different experimental conditions [Table 2 (entries I-VI) and Scheme 2]. When trans-[PdCl2(dmso)2] was treated with the equimolecular amount of ligand 1a or a two-fold excess in refluxing methanol for 1 h, a pale yellowish precipitate (hereinafter referred to as 2a) was formed with a yield of 28% in the case of using a molar ratio of 1:1 (Table 2, entry I). Elemental analyses of 2a and NMR characterization

420 agreed with those expected for trans-[PdCl2(1a)2]. Molecular models suggest that a cisdisposition of the

421 ligands will introduce strong steric hindrance between the two close carbazole ligands 1a and on this

422 basis, we assume that the isolated solid is the trans- isomer. Compounds [PdX2(L)2] with bulky

423 monodentate N-donor ligands, including heterocycles such as benzothiazolyl derivatives, tend to adopt

424 this configuration in solution and in the solid state [93–95]. Compound 2a is a stable solid at room

425 temperature and exhibits low solubility in CHCl3 or CH2Cl2. Compound 2a can be obtained with a

426 higher yield of 82% and at room temperature using Na2[PdCl4], instead of the trans-[PdCl2(dmso)2], a

427 two-fold excess of carbazole 1a and methanol as solvent (Table 2, entry II).

428 In order to compare the effect of the binding of the M(II) ion to the carbazole 1a on the anticancer

429 activity, we also studied the reactivity of 1a in front of Pt(II). Treatment of equimolar amounts of 1a and

430 cis- [PtCl2(dmso)2] in methanol (HPLC grade) under reflux for 1 h, followed by the work-up of a SiO2

431 column chromatography gave a yellowish solid (3a) (Table 2, entry III and Scheme 2). Its elemental

432 analyses were consistent with those expected for [PtCl2(1a)(dmso)]. Moreover, the position of the

433 singlet observed in the 195Pt{1H}-NMR spectrum of 3a (δ=−2983 ppm) agrees with those of related

434 Pt(II) complexes with a "PtCl2(Nheterocycle)(Sdmso)" core [57–59,96–98]. Its 1H-NMR spectrum

435 (Fig. S2) showed two singlets of relative intensities 1:2 in the high field region. The less intense one is

436 assigned to the methylic protons of the ligand at δ=4.0 ppm; while the other corresponds to the six

437 protons of the dmso ligand. This finding is characteristic of trans- isomers of [PtCl2(N-donor

438 ligand)(dmso)] [57–59,96–98], thus indicating that compound 3a is trans-[PtCl2(1a)(dmso)]. It should

439 be noted that when the reaction was performed using longer reaction times no evidences of the

440 formation of any other Pt(II) compound were detected by 1H-NMR.

441 Since it is well-known that the presence of a base such as NaOAc and mixtures of toluene / methanol

442 (5:1) as solvent may induce the formation of the cis- isomers of compounds [PtCl2(N-donor

443 ligand)(dmso)] or even cycloplatinated complexes [57–60,96–101], we also investigated whether for

444 ligand 1a the addition of NaOAc could affect the nature of the final Pt(II) product. When equimolar

445 amounts of 1a, cis-[PtCl2(dmso)2] and NaOAc were refluxed in a mixture of toluene: methanol (5:1) for

446 72 h (Table 2, entry VI and Scheme 2), the 1H-NMR spectrum of the raw material in CDCl3 at 298 K

447 (Fig. S4) revealed the coexistence of 3a and a minor product (hereinafter referred to as 4a). The work-up

448 of a column chromatography allowed us to isolate complex 3a and a solid containing a mixture of 3a

449 and 4a. The 195Pt{1H} NMR spectrum of the solid dissolved in CDCl3 at 298 K (Fig. S1, A) showed

450 two singlets (one at δ=−2980 ppm (due to 3a) and the other at δ = −2932 ppm assigned to compound

451 4a). Their chemical shifts suggest that the environment of the Pt(II) atoms in 3a and 4a should be very

452 similar. Moreover, the separation between the two singlets (ca. 41 ppm), falls in the typical range

453 reported for trans- and cis- isomers of [Pt(N-donor)Cl2(dmso)] compounds. Besides that, its 1H-NMR

454 spectrum (Fig. S1, B) revealed that for 4a the resonances due to the protons of the dmso ligand appeared

455 as two singlets, in good agreement with a cisdisposition of the Cl− ligands. On these basis we assumed

456   that 4a is the cis- isomer of [PtCl2(1a)(dmso)]. Unfortunately, attempts to isolate 4a in its pure form, by

457   fractional crystallization or subsequent column chromatography failed.

458   Comparison of 1H-NMR spectra of the new complexes (2a, 3a and 4a) with that of the parent ligand 1a

459   reveals that the resonances due to the H2 and H4 protons of the carbazole array were highly affected by

460   the binding of the nitrogen to the Pt(II) ion. It should be noted that: a) the formation of the Pt-

461   N(thiazole) bond requires the cleavage of the intramolecular C11eH12⋯N hydrogen bond, b) in cis- and

462   trans- isomers of [PtCl2(N-heterocycle)(dmso)] complexes, the heterocycle is orthogonal to the main

463   coordination plane of the ligand [57–60,93,102,103], and c) frequently ancillary ligands (Cl− or dmso)

464   are involved in additional CeH ⋯X [X=Cl or O(dmso)] contacts with the neutral N-donor ligand

465   [93,102,103]. All these findings could explain the variations observed in the chemical shifts of the

466   protons adjacent to position 3 in complexes 3a and 4a.

467   In order to compare the potential coordination ability of the two new carbazoles, the reactivity of the

468   thienyl derivative 1b with [MCl2(dmso)2] and Na2[PdCl4] was studied under identical conditions as for

469   1a (described above and shown in Scheme 2) and using identical conditions as those shown in Table 2

470   (entries I - IV). However, none of these studies allowed us neither the isolation or even the detection by

471   1H-NMR of any Pd(II) or Pt(II) complex, thus suggesting that thiazolesubstituted carbazole 1a has a

472   greater coordination ability than the thienyl analogue 1b.

473

474   3.2. Electronic spectra and optical properties

475   Absorption spectra of CH2Cl2 solutions of 1a and 1b at 298 K (Table 3 and Fig. S5, A) showed two

476   intense bands in the range 250–450 nm that are characteristic of carbazoles. The corresponding UV–vis

477   spectra of the complexes 2a and 3a (Fig. S5, B and Table 3) exhibited two intense absorption bands in

478   the range $300{\leq}\lambda < 350$ nm. One of them shifted to lower energies in relation to the free ligand being for

479   the Pt(II) complex (3a) the magnitude of the shift bigger than for the Pd(II) complex 2a (Table 3). These

480   findings suggest that this absorption band is due to a metal perturbed intraligand electronic transition

481   (MPILET). The second absorption band, at higher energies, is practically coincident with that of the free

482   ligand. The spectra of compounds 2a and 3a (Fig. S5, B) also exhibited an additional and poorly

483   resolved absorption band at lower wavelengths $[280{\leq}\lambda < 290$ nm].

484   The emission spectra of 1a, 1b, 2a and 3a were recorded in CH2Cl2 solution at 298 K. Upon excitation

485   at λexc=300 nm, the free ligands 1a and 1b exhibited emission bands in the range 370–395 nm (Fig. S6

486   and Table 3). The thienyl-based derivative 1b showed a bathochromic shift of the wavelength of

487   maximum emission of 10 nm in comparison to the thiazolyl-based ligand 1a, according to the strongest

488   electron-donating character of the thienyl unit. It should be noted that the quantum yield of 1a (Table 3)

489   is significantly higher than that of 1b. Complexes 2a and 3a exhibited also emission bands consistent

490   with that of ligand 1a, but their fluorescence quantum yields [104] decreased considerably in relation to

491   the free ligand (1a).

492

493   3.3. Computational studies

494   In order to elucidate the effect produced by the thiazolyl or thienyl groups of compounds 1a and 1b on

495   the electronic delocalization, computational calculations based on the density functional theory (DFT)

496   methodology were undertaken [68]. Calculations were carried out using the B3LYP hybrid functional

497   [69,70] and the 6-31G* basis set [72,73] implemented in the Gaussian03 program [71]. In a first stage,

498   geometries of compounds 1a and 1b were optimized without imposing any restriction. Final atomic

499   coordinates for the optimized geometries are included as supplementary information (Tables S1–S2).

500   Bond lengths and angles of the optimised geometry of 1a were consistent with those obtained from the

501   X-ray studies (the differences did not clearly exceed 3σ) and those of 1b are in the range reported for

502   related carbazoles with mono or polythienyl units on position 3 [50–52,93,103].

503   Molecular orbital (MO) calculations of the optimized geometries revealed that highest occupied

504   molecular orbital (HOMO) (Fig. 5) of 1a and 1b are very similar except for a tiny difference in the

505   contribution of the atomic orbitals of the sulphur atom. The LUMO (Fig. 5) of 1a is mainly centred on

506   the thiazolyl unit and two of the rings of the carbazole; while in 1b, the contribution of the thienyl

507   decreases in relation to that of the thiazole in 1a. Moreover, the HOMO-LUMO gap (ΔE) of 1b (4.32

508   eV) is higher than for 1a (4.14 eV). These findings suggest that the replacement of the thiazolyl ring of

509   1a by the thienyl in 1b reduces the electronic delocalization mentioned above.

510   In the optimized geometry of 1b the intramolecular separation between the S1 atom and the hydrogen

511   atom of phenyl ring (2.848 Å) is larger than in 1a [S1···H: 2.748 Å (optimized geometry) or 2.751 Å

512   (from the crystal structure)] and the angle formed by the heterocycle and the carbazole is 30.3° bigger

513   than in 1a. Since it is well-known that deviations from planarity affects the electronic delocalization, the

514   properties of the compounds and their potential utility, we also calculated the energy of the molecules

515   for different orientations of the attached heterocycle versus the carbazole unit using molecular

516   mechanics. These arrangements were generated by modifying the torsion angle defined by the set of

517   atoms S1-C2'-C3-C4 (hereinafter referred to as φ) from 0° to 360°. The results shown in Fig. 6, reveal

518   that for 1a the minimum energy corresponds to φ values in the ranges ($0° \leq \varphi \leq 16°$ and $344° \leq \varphi \leq 360°$),

519   that is to say close to co-planarity, similar to that found in the crystal structure $\varphi=13.5°$ and with the S1

520   atom and NMe group located in opposite sides.

521   The energy barrier to achieve an orthogonal arrangement of the thiazole ($\varphi=90°$ or 270°) is rather high

522   (9.1 kJ/mol). The conformer with the N1 and N2 atoms on opposite sides, [φ values between 164° and

523   196°] is slightly less stable than for $\varphi=0 \pm 16°$ (Fig. 6). The differences between the energies of both

524   conformers determined from molecular mechanics calculations and DFT are 0.4 and 0.5 Kcal/mol,

525   respectively.

526   In contrast with the results obtained for 1a, in 1b the most favourable orientation of the thienyl unit is far

527   away from co-planarity and corresponds to φ values in the ranges 128°–133° and 232°–237°. The

528   energy barriers to achieve coplanar arrangements (Fig. 6) are smaller than that obtained for 1a (9.1

529   kJ/mol); consequently, from an energetic point of view, the free rotation of the thienyl unit, that requires

530 a smaller energy income, is more likely to occur than that of the thiazolyl ring of 1a. In addition, time

531 dependent DFT (TD-DFT) calculations were performed to achieve the assignment of the bands observed

532 in the UV–vis spectra (Table S4 and Fig. S7).

533 Besides that and in order to compare the stability of the two isomers of the platinum(II) complexes (3a

534 and 4a), we optimized their geometries (Tables S5 and S6) and afterwards we calculated their relative

535 energies. The results revealed (Table S7) that in vacuum the transisomer (3a) is ca. 4.3 kcal/mol more

536 stable than 4a (cis- isomer), but in methanol (MeOH) the difference between their calculated free

537 energies decreased to −0.30 kcal/mol. This may explain the formation of both isomers in a similar molar

538 ratio.

539

540 3.4. Biological studies

541 3.4.1. Antiproliferative assay

542 We have evaluated the cytotoxic activity of ligands 1a and 1b and the new complexes 2a and 3a in front

543 of the colon cell line HCT116 and two breast cancer cell lines [the triple negative (ER, PR and no HER2

544 over expression) MDA-MB231 and the MCF7]. The effects of the new products on the growth of the

545 three cell lines and that of cisplatin, used as positive control, were assessed after 72 h and the results are

546 presented in Table 4 and Fig. 7.

547 The comparison of the in vitro cytotoxic activities of the free carbazoles 1a and 1b in the HCT116 cell

548 line revealed that the replacement of the thienyl ring (in 1b) by the thiazolyl unit of 1a produced a

549 significant enhancement of the cytotoxic potency. This trend is practically identical to those observed in

550 the two breast (MDA-MB231 and the MCF7) cancer cell lines and could be attributed to several factors.

551 One of these could be the lipophilicity that, as shown in Table 4, is expected to be slightly different for

552 the two systems. It should be noted that in the MCF7 cell line ligand 1a is (ca. 9.5 times) more potent

553 than cisplatin, the non-alkylated 9H-carbazole (IC50 > 40μM) and similar to doxorubicin (IC50=2.3 μM

554 [105] or 2.43 ± 0.24 μM [106]).

555 In order to compare the effect produced by the binding of the Pd(II) or Pt(II) we also examined the

556 effect produced by the complexes 2a and 3a on identical cell lines. As shown in Table 4 and Fig. 7, the

557 Pd(II) complex 2a did not show any relevant antiproliferative activity (IC50 > 100 μM) in the HCT116

558 and MDA-MB231 cell lines. In the MCF7 it was more active, but its potency was close (IC50=24 ± 2

559 μM) to that of cisplatin (IC50=19 ± 4.5 μM). In contrast, the Pt(II) complex (3a) exhibited a higher

560 inhibitory growth effect, being 9 times more potent than the reference drug in the MCF7 breast cancer

561 cell line.

562 It is well-known that the preparation of new products with improved cytotoxic potency is not the unique

563 requirement in medicinal chemistry and drug design, other factors such as the lipophilicity that

564 contributes to the ADMET (absorption, distribution, metabolism excretion and toxicity) properties of

565 drugs also plays a crucial role. Nowadays, the lipophilic efficiency (LipE) index [107–110] that includes

566 lipophilicity and potency is becoming more and more popular in drug design and optimization, because

567 it allows to normalize the observed potency with changes in the lipophilicity.

568 In view of this, we calculated the Clog P values for the new compounds and their LipE index in the

569 MCF7 cell line. The results (Table 4) reveal that for the compounds characterized in this work the LipE

570 index increases as follow 2a≪1b < 1a≤3a. The Pd(II) complex 2a that shows low solubility it is

571 simultaneously the most lipophilic and the less potent compound of the series. In contrast with these

572 results, for the carbazole-thiazole ligand 1a and its trans-[PtCl2(1a)(dmso)] complex 3a there is an

573 effective combination of their cytotoxic potency in MCF7 and lipophilicity, and on these basis they are

574 promising scaffolds in the search of optimized drugs. Chemical modifications of the core of ligand 1a,

575 its binding to the Pt(II) atom or even changes on the ancillary ligands bound to it in 3a may allow to tune

576 the lipophilicity and to improve the lipophilic efficiency.

577

578

579 3.4.2. Additional studies to elucidate the mechanism of action

580 In the majority of the described cases of cytotoxic carbazoles, they act as DNA-intercalators or as

581 Topoisomerase I/II (or telomerases) inhibitors [24,111], although other mechanisms of action involving

582 different targets {i.e. estrogen receptors (ER) or cyclin dependent kinases (CDK), among others} have

583 also been postulated [22–26,112]. To examine whether the presence of the thiazole (in 1a) or the thienyl

584 unit (in 1b) in the free ligand and the binding of 1a to the Pd(II) or Pt(II) ions in complexes 2a and 3a,

585 could have an important role in the mechanism of action, additional experiments were performed.

586 To elucidate whether compounds 1a, 1b, 2a and 3a act as DNA intercalators or as Topoisomerase I or II

587 inhibitors, three different sets of experiments were undertaken. In a first stage it was examined if the

588 new compounds could induce changes in the electrophoretic mobility of the supercoiled closed form

589 (ccc) of pBluescript SK+ plasmid DNA. For DNA migration studies, the plasmid was incubated with

590 compounds 1a, 1b, 2a and 3a at increasing concentrations ranging from 0 to 200 μM. For comparison

591 purposes, incubation of DNA with cisplatin or ethidium bromide (EB) was also performed. As expected,

592 cisplatin greatly altered the electrophoretic mobility of pBluescript DNA at all concentrations tested. As

593 depicted in Fig. 8, the free ligands (1a and 1b) and the Pd(II) compound (2a) were not effective. Only

594 the Pt(II) complex (3a) produced a significant effect on the electrophoretic mobility of native

595 pBluescript DNA at concentrations>100 μM. Secondly, a Topoisomerase based gel assay was performed

596 to evaluate the ability of compounds 1a, 1b, 2a and 3a to intercalate into DNA or to act as DNA

597 Topoisomerase I inhibitors. For that, supercoiled pBluescript plasmid DNA was incubated with

598 Topoisomerase I in the presence of increasing concentrations of the compounds under study. The results

599 are presented in Fig. 9, where ethidium bromide (EB) was used as an intercalator control. The analysed

600 compounds did not prevent unwinding of DNA indicating that they are neither intercalators nor

601 Topoisomerase I inhibitors.

As mentioned above, another important target for anticancer agents is the Topoisomerase II, which is associated with solving the topological constraints of DNA by transiently cleaving both strands of the double helix [24,111]. In humans there are two Topoisomerase II isoenzymes, IIα and IIβ. Here we study the capability of compounds 1a, 1b, 2a and 3a as catalytic inhibitors of Topoisomerase IIα. The inhibitory activity was evaluated by measuring the extent of enzyme mediated relaxed DNA after treatment with 100 μM of 1a, 1b, 2a and 3a compounds. Only the Pd(II) complex 2a showed at this concentration inhibitory activity (Fig. 10A). The inhibitory effect of 2a was further examined at different concentrations, from 50 to 200 μM. As it is shown in Fig. 10B, compound 2a showed inhibition at 100 μM but not at 50 μM.

Other mechanism of action implies Cathepsin B, which is a cysteine metaloprotease that could be involved in metastasis, angiogenesis and tumour progression. Examples of Pd(II) and Pt(II) complexes as inhibitors of Cathepsin B have been reported [113]. However, none of the new compounds presented in this work (1a, 1b, 2a and 3a) inhibited the enzyme activity at 100 μM concentration.

Overall the biological studies undertaken with the new compounds 1a, 1b, 2a and 3a provide conclusive evidences. The DNA migration studies revealed that only Pt(II) complex (3a) modifies the electrophoretic mobility of the plasmid in a similar way as cisplatin but at higher concentrations. Experimental results also revealed that neither compounds 1a, with higher cytotoxic activity than cisplatin in the tested cancer lines HCT116 and MCF7, nor compounds 1b or 2a operate as intercalators and none of them are inhibitors of Topoisomerase I or cathepsin B. However, the Pd(II) complex (2a) inhibits the activity of Topoisomerase IIα (at 200 μM concentration).

All the new compounds show lower toxicity on the normal and nontumoral human skin fibroblast BJ cell line than cisplatin (Table 4). Among the new compounds, 1a and its Pt(II) complex 3a are the most active in the assayed HCT116, MDA-MB231 and MCF7 cancer cell lines. Moreover, compound 1a, clearly more potent than 3a, has additional interest because it does not contain Pt(II) and consequently might not produce the typical and undesirable side effects of conventional Pt(II)-based drugs. In addition, compound 1a shows a remarkable high stability in the solid state and also in dmso or in mixtures dmso: D2O (Figs. S9–S15) at 298 K. These findings enhance the interest and relevance of carbazole 1a for further and additional biological studies.

4. CONCLUSIONS

Here we have presented two new N-methylated and 3-substituted carbazoles with a thiazolyl (1a) or a thienyl (1b) unit and comparative studies of their properties and reactivity in front of Na2[PdCl4] or [MCl2(dmso)2] {trans- for M=Pd or cis- for M=Pt} and biological activities. The obtained results proved that compound 1a is clearly more reactive than 1b and has a greater coordination capability towards the Pd(II) and Pt(II) ions, leading to trans-[PdCl2(1a)2] (2a) and the geometrical isomers {trans-(3a) or cis-(4a)} of [PtCl2(1a)(dmso)]. DFT studies confirmed the different reactivity of 1a and 1b and the formation of the isomers 3a and 4a.

In vitro studies on the cytotoxic activity of compounds 1a, 1b, 2a and 3a in the cancer cell lines (HCT116, MDA-MB231 and MCF7) and in the normal and non-tumoral human skin fibroblasts BJ cell line show that: a) the replacement of the thiazole (of 1a) by the thienyl (to give 1b) reduces the inhibitory growth effect, b) the binding of 1a to the Pt (II) atom (3a) reduces its cytotoxic activity, c) compound 2a is less active than the Pt(II) complex 3a and d) all compounds are less toxic than cisplatin in the BJ cell line. Additional biological studies revealed that: a) only the Pt(II) complex (3a) induced significant changes on the electrophoretic mobility of the pBluescript DNA, but at higher concentrations than the cisplatin and b) neither the ligands (1a and 1b) nor the Pd(II) (2a) or Pt(II) complex (3a) acted as intercalators or inhibitors of Topoisomerase I or Cathepsin B. However, the Pd(II) complex (2a) with an inhibitory growth activity in the MCF7 cell line similar to that of cisplatin inhibited the Topoisomerase IIα activity. These findings suggest that the binding of the Pd(II) or the Pt(II) to the carbazole 1a not only produces significant changes in their cytotoxic activity but also on their mechanism of action.

To sum up, among the new compounds, 1a with high stability, low toxicity, potent cytotoxic activity and photophysical properties is an excellent candidate for further studies on: a) their effect on a wider panel of cancer cell lines, b) its mechanism of action, c) its potential use in combined therapies even in photodynamic therapy, and d) other biological activities (i.e. antibacterial, antifungal, etc.) maybe relevant in new drug design and development.

660   **ACKNOWLEDGEMENTS**

661

664

APPENDIX A. SUPPLEMENTARY DATA

Tables containing: final atomic coordinates of the optimised geometries of carbazoles 1a and 1b (Tables S1 and S2, respectively), calculated energies of the HOMO and LUMO orbitals, energy gaps for the new carbazoles and calculated values of the Mulliken charges of selected atoms (Table S3), summary of the results obtained from the computational studies showing electronic transitions with greater contributions in the absorption bands for 1a and 1b (Table S4), calculated final atomic coordinates for isomers 3a and 4a (Tables S5–S6) and calculated energies for 3a and 4a (Table S7) and additional Figures (Figs. S1–S12) showing: the 1H-NMR spectrum of compound 3a (Fig. S2); an expansion of the 1H-NMR spectrum of the raw material obtained after 24 h under reflux, showing the presence of complex 3a and another minor product (Fig. S3); the 1H-NMR spectrum of the crude material obtained after 72 h that shows the coexistence of 3a and an additional product 4a (Fig. S4); The 195Pt{1H} and 1H-NMR spectra of the mixture of the two isomers of [PtCl2(1a)(dmso)] {trans- (3a) and cis-(4a)}, isolated from the column (Fig. S1); UV–Vis spectra of compounds 1a, 1b, 2a and 3a (Fig. S5), emission spectra of compounds 1a, 1b, 2a and 3a (Fig. S6); calculated absorption spectra of compounds 1a and 1b (Fig. S7); the HOMO−1 and LUMO+1 orbitals for carbazoles 1a and 1b (Fig. S8); Figures (Figs. S9–S12); showing the 1H-NMR spectra of a freshly prepared solution of compound 1a in dmso-d6 (Fig. S9) or in mixtures dmso-d6: D2O (from 4:1 to 1:1) (Figs. S10–S12) after several periods of storage at 298 K; the 1H-NMR spectra of a freshly prepared solution of compounds 1b, 2a and 3a in dmso-d6 after several periods of storage at 298 K (Figs. S13–S15); and ESI-MS spectra of compounds 1a, 1b and 3a (Figs. S16–S18). Supplementary data to this article can be found online at https://doi.org/10.1016/j.jinorgbio.2018.03.008.

REFERENCES

[1]   Cancer Facts & Figures 2017, American Cancer Society, 2017, http://www.cancer. org/research/cancerfactsstatistics/cancerfactsfigures2017/index , Accessed date: May 2017.

[2]   Cancer statistics center, American Cancer Society, https://cancerstatisticscenter. cancer.org/?_ga=1.48498790.1307978637.1460725255#/, (2017) , Accessed date: May 2017.

[3]   A.B. Ryerson, C.R. Eheman, S.F. Altekruse, J.W. Ward, A. Jemal, R.L. Sherman, S.J. Henley, D. Holtzman, A. Lake, A.-M. Noone, R.N. Anderson, J. Ma, K.N. Ly, K.A. Cronin, L. Penberthy, B.A. Kohler, Cancer 122 (2016) 1312–1337.

[4]   Updated Information on Colorectal and Breast Cancer can be Obtained from the American Cancer Society, Atlanta, Georgia, USA (http://www.cancer.org/acs) Through (a) www.cancer.org/acs/groups/content/documents/document/acspc- 042280.pdf and (b) www.cancer.org/acs/groups/content/documents/document/ acspc-04638.pdf (for Colorectal Cancer and Breast Cancer, Respectively) (2017) (accessed May 2017).

[5]   G.F. Weber, Molecular Therapies of Cancer, Springer, Germany, 2015.

[6]   A.C. Flick, H.X. Ding, C.A. Leverett, R.E. Kyne Jr., K.K.-C. Liu, S.J. Fink, C.J. O'Donnell, Bioorg. Med. Chem. 24 (2016) 1937–1980.

[7]   N.A. Meanwell, Chem. Res. Toxicol. 29 (2016) 564–616.

[8]   A.L. Harvey, R.L. Clark, S.P. Mackay, B.F. Johnston, Expert Opin. Drug Discovery 5 (2010) 559–568.

[9]   E.A.G. Blomme, Y. Will, Chem. Res. Toxicol. 29 (2016) 473–504.

[10]   S.A. McKie, Future Med. Chem. 8 (2016) 579–602.

[11]   I. Ali, M.N. Lone, Z.A. Al-Othman, A. Al-Warthan, M.M. Sanagi, Curr. Drug Targets 16 (2015) 711–734.

[12]   A.R. Katritzky, C.A. Ramsden, E.F.V. Scriven, R.J.K. Taylor (Eds.), Comprehensive Heterocyclic Chemistry III, Elsevier, Oxford (UK), 2008.

[13]   R.K. Parashar, Chemistry of Heterocyclic Compounds, CRC Press, 2014.

713 [14] A.F. Pozharskii, A.T. Soldatenkov, A.R. Katritzky, Heterocycles in Life and Society: An
714 Introduction to Heterocyclic Chemistry, Biochemistry and Applications, second ed., Wiley-
715 VCH, Weinheim (Germany), 2011.

716 [15] J.A. McCleverty, T.J. Meyer (Eds.), Comprehensive Coordination Chemistry II: From Biology
717 to Nanotechnology, Elsevier, Amsterdam, 2003.

718 [16] R.H. Crabtree, D.M.P. Mingos (Eds.), Comprehensive Organometallic Chemistry III, second
719 ed., Elsevier, Oxford, UK, 2007.

720 [17] G. Wilkinson, R.D. Gillard, J.A. McCleverty (Eds.), Comprehensive Coordination Chemistry:
721 The Synthesis, Reactions, Properties and Applications of Coordination Compounds, Pergamon
722 Press, Oxford, UK, 1987.

723 [18] J.J. Li, Heterocyclic Chemistry in Drug Discovery, John Wiley & Sons, Hoboken, USA, 2013.

724 [19] T.Y. Zhang, Chapter one - the evolving landscape of heterocycles in drugs and drug candidates,
725 in: E.F.V. Scriven, C.A. Ramsden (Eds.), Advances in Heterocyclic Chemistry, 121 Academic
726 Press, 2017, pp. 1–12.

727 [20] A. Gomtsyan, Chem. Heterocycl. Compd. 48 (2012) 7–10.

728 [21] P. Martins, J. Jesús, S. Santos, L.R. Raposo, C. Roma-Rodrigues, P.V. Baptista, A.R. Fernandes,
729 Molecules 20 (2015) 16852–16891.

730 [22] L.S. Tsutsumi, D. Gündisch, D. Sun, Carbazole scaffold in medicinal chemistry and natural
731 products: a review from 2010–2015, Curr. Top. Med. Chem. 16 (2016) 1290–1313.

732 [23] K.N. Mounika, A.N. Jyothy, G.N. Raju, R.R. Nadendla, World J. Pharm. Pharm. Sci. 4 (2015)
733 420–428.

734 [24] M. Bashir, A. Bano, A.S. Ijaz, B.A. Chaudhary, Molecules 20 (2015) 13496–13517.

735 [25] C. Asche, M. Demeunynck, Anti Cancer Agents Med. Chem. 7 (2007) 247–267.

736 [26] A. Caruso, D. Iacopetta, F. Puoci, A.R. Cappello, C. Saturnino, M.S. Sinicropi, Mini-Rev. Med.
737 Chem. 16 (2016) 630–643.

738 [27] T. Paneer, G. Saravanan, M. Palanivelu, Anticancer Evaluation of Thiazole Based Heterocycles
739 - A Review, Lambert Academic Publishing, Saarbrücken, Germany, 2014.

740 [28] A. Ayati, S. Emami, A. Asadipour, A. Shafiee, A. Foroumadi, Eur. J. Med. Chem. 97 (2015)
741 699–718.

742 [29] A. Chawla, H. Kaur, P. Chawla, U.S. Baghel, J. Glob. Trends Pharm. Sci. 5 (2014) 1641–1648.

743 [30] A. Leoni, A. Locatelli, R. Morigi, M. Rambaldi, Expert Opin. Ther. Pat. 24 (2014) 201–216.

744 [31] K.K. Jha, S. Kumar, I. Tomer, R. Mishra, J. Pharm. Res. 5 (2012) 560–566.

745 [32] M.M. Ghorab, M.S. Bashandy, M.S. Alsaid, Acta Pharma. 64 (2014) 419–431.

746 [33] D. Gramec, L.P. Mašič, M.S. Dolenc, Chem. Res. Toxicol. 27 (2014) 1344–1358.

747 [34] N.C. Garbett, D.E. Graves, Curr. Med. Chem. Anticancer Agents 4 (2004) 149–172.

748 [35] C.M. Miller, F.O. McCarthy, RSC Adv. 2 (2012) 8883–8918.

749 [36] R.K. Mehmood, Oncol. Rev. 8 (2014) 256.

750 [37] F.M. Muggia, A. Bonetti, J.D. Hoeschele, M. Rozencweig, S.B. Howell, J. Clin. Oncol. 33
751 (2015) 4219–4226.

752 [38] S. Amptoulach, N. Tsavaris, Chemother. Res. Pract. (2011) 843019, , http://dx.
753 doi.org/10.1155/2011/843019.

754 [39] M.A. Jordan, Curr. Med. Chem. Anticancer Agents 2 (2002) 1–17.

755 [40] K. Chatterjee, J. Zhang, N. Honbo, J.S. Karliner, Cardiology 115 (2010) 155–162.

756 [41] F. Trudu, F. Amato, P. Vanhara, T. Pivetta, E.M. Peña-Méndez, J. Havel, J. Appl. Biomed. 13
757 (2015) 79–103.

758 [42] H. Jiang, J. Sun, J. Zhang, Curr. Org. Chem. 16 (2012) 2014–2025.

759 [43] M. Reig, G. Bagdziunas, D. Volyniuk, J.V. Grazulevicius, D. Velasco, Phys. Chem. Chem.
760 Phys. 19 (2017) 6721–6730.

761 [44] M. Reig, C. Gozálvez, R. Bujaldón, G. Bagdziunas, K. Ivaniuk, N. Kostiv, D. Volyniuk, J.V.
762 Grazulevicius, D. Velasco, Dyes Pigments 137 (2017) 24–35.

763 [45] M. Reig, G. Bubniene, W. Cambarau, V. Jankauskas, V. Getautis, E. Palomares, E. Martínez-
764 Ferrero, D. Velasco, RSC Adv. 6 (2016) 9247–9253.

765   [46]   M. Reig, J. Puigdollers, D. Velasco, J. Mater. Chem. C 3 (2015) 506–513.

766   [47]   J.L. Díaz, A. Dobarro, B. Villacampa, D. Velasco, Chem. Mater. 13 (2001) 2528–2536.

767   [48]   B.-B. Ma, Y.-X. Peng, T. Tao, W. Huang, Dalton Trans. 43 (2014) 16601–16604.

768   [49]   Y.-X. Li, X.-T. Tao, F.-J. Wang, T. He, M.-H. Jiang, Org. Electron. 10 (2009) 910–917.

769   [50]   S.-I. Kato, S. Shimizu, A. Kobayashi, T. Yoshihara, S. Tobita, Y. Nakamura, J. Org. Chem. 79
770   (2014) 618–629.

771   [51]   S.-I. Kato, S. Shimizu, H. Taguchi, A. Kobayashi, S. Tobita, Y. Nakamura, J. Org. Chem. 77
772   (2012) 3222–3232.

773   [52]   P. Wang, Y. Ju, S.Y. Tang, J.Y. Wu, H.P. Zhou, Acta Cryst., Sect. E 63 (2007) o3671.

774   [53]   M.A.T. Nguyen, A.K. Mungara, J.-A. Kim, K.D. Lee, S. Park, Phosphorus Sulfur Silicon Relat.
775   Elem. 190 (2015) 191–199.

776   [54]   M.S. Shaikh, M.B. Palkar, H.M. Patel, R.A. Rane, W.S. Alwan, M.M. Shaikh, I.M. Shaikh,
777   G.A. Hampannavar, R. Karpoormath, RSC Adv. 4 (2014) 62308–62320.

778   [55]   M.H. Adbel-Kader (Ed.), Photodynamic Therapy from Theory to Applications, Springer,
779   Heildelberg, Germany, 2014.

780   [56]   J.U. Chukwu, C. López, A. González, M. Font-Bardía, M.T. Calvet, R. Messeguer, C. Calvis, J.
781   Organomet. Chem. 766 (2014) 13–21.

782   [57]   E. Guillén, A. González, C. López, P.K. Basu, A. Ghosh, M. Font-Bardía, C. Calvis, R.
783   Messeguer, Eur. J. Inorg. Chem. (2015) 3781–3790.

784   [58]   A. González, J. Granell, C. López, R. Bosque, L. Rodríguez, M. Font-Bardía, T. Calvet, X.
785   Solans, J. Organomet. Chem. 726 (2013) 21–31.

786   [59]   M. Tomé, C. López, A. Gonzalez, B. Ozay, J. Quirante, M. Font-Bardía, T. Calvet, C. Calvis, R.
787   Messeguer, L. Baldomà, J. Badia, J. Mol. Struct. 1048 (2013) 88–97.

788   [60]   C. López, A. González, R. Bosque, P.K. Basu, M. Font-Bardía, T. Calvet, RSC Adv. 2 (2012)
789   1986–2002.

790   [61]   Z. Szafran, R.M. Pike, M.M. Singh, Microscale Inorganic Chemistry, A Comprehensive
791   Laboratory Experience, John Wiley & Sons, New York, USA, 1991, p. 218.

792   [62]   J.H. Price, A.N. Williamson, R.F. Schramm, B.B. Wayland, Inorg. Chem. 11 (1972) 1280–
793   1284.

794   [63]   S.H. Tucker, J. Chem. Soc. 129 (1926) 546–553.

795   [64]   D.D. Perrin, W.L.F. Armarego, Purification of Laboratory Chemicals, fourth ed., Butterworth–
796   Heinemann, Oxford, UK, 1996.

797   [65]   G.M. Sheldrick, Acta Cryst A64 (2008) 112–122.

798   [66]   T.A. Halgren, J. Comput. Chem. 17 (1996) 490–519.

799   [67]   Spartan '14 v. 1.1.0, Wavefunction, Inc, Irvine, CA, USA, 2013.

800   [68]   P. Hohenberg, W. Kohn, Phys. Rev. 136 (1964) B864–B871.

801   [69]   A.D. Becke, J. Chem. Phys. 98 (1993) 5648–5652.

802   [70]   C. Lee, W. Yang, R.G. Parr, Phys. Rev. B 37 (1988) 785–789.

803   [71]   M.J. Frisch, G.W. Trucks, H.B. Schlegel, G.E. Scuseria, M.A. Robb, J.R. Cheeseman, J.A.
804   Montgomery, T. Vreven, K.N. Kudin, J.C. Burant, J.M. Millam, S.S. Iyengar, J. Tomasi, V.
805   Barone, B. Mennucci, M. Cossi, G. Scalmani, N. Rega, G.A. Petersson, H. Nakatsuji, M. Hada,
806   M. Ehara, K. Toyota, R. Fukuda, J. Hasegawa, M. Ishida, T. Nakajima, Y. Honda, O. Kitao, H.
807   Nakai, M. Klene, X. Li, J.E. Knox, H.P. Hratchian, J.B. Cross, V. Bakken, C. Adamo, J.
808   Jaramillo, R. Gomperts, R.E. Stratmann, O. Yazyev, A.J. Austin, R. Cammi, C. Pomelli, J.W.
809   Ochterski, P.Y. Ayala, K. Morokuma, G.A. Voth, P. Salvador, J.J. Dannenberg, V.G.
810   Zakrzewski, S. Dapprich, A.D. Daniels, M.C. Strain, O. Farkas, D.K. Malick, A.D. Rabuck, K.
811   Raghavachari, J.B. Foresman, J.V. Ortiz, Q. Cui, A.G. Baboul, S. Clifford, J. Cioslowski, B.B.
812   Stefanov, G. Liu, A. Liashenko, P. Piskorz,I. Komaromi, R.L. Martin, D.J. Fox, T. Keith, M.A.
813   Al-Laham, C.Y. Peng, A. Nanayakkara, M. Challacombe, P.M.W. Gill, B. Johnson, W. Chen,
814   M.W. Wong, C. Gonzalez, J.A. Pople, Gaussian 03 (Revision C.02), Gaussian, Inc, Wallingford,
815   CT, 2004.

816   [72]   P.C. Hariharan, J.A. Pople, Theor. Chim. Acta 28 (1973) 213–222.

817   [73]   M.M. Francl, W.J. Pietro, W.J. Hehre, J.S. Binkley, M.S. Gordon, D.J. DeFrees, J.A. Pople, J.
818   Chem. Phys. 77 (1982) 3654–3665.

819   [74]   K.T. Givens, S. Kitada, A.K. Chen, J. Rothschiller, D.A. Lee, Invest. Ophthalmol. Vis. Sci. 31
820   (1990) 1856–1862.

821 [75] A. Abdullah, F. Huq, A. Chowdhury, H. Tayyem, P. Beale, K. Fisher, BMC Chem. Biol. 6
822 (2006) 3.

823 [76] D.S. Sappal, A.K. McClendon, J.A. Fleming, V. Thoroddsen, K. Connolly, C. Reimer, R.K.
824 Blackman, C.E. Bulawa, N. Osheroff, P. Charlton, L.A. Rudolph-Owen, Mol. Cancer Ther. 3
825 (2004) 47–58.

826 [77] A. Casini, C. Gabbiani, F. Sorrentino, M.P. Rigobello, A. Bindoli, T.J. Geldbach, A. Marrone,
827 N. Re, C.G. Hartinger, P.J. Dyson, L. Messori, J. Med. Chem. 51 (2008) 6773–6781.

828 [78] M.E. Monge, S.M. Bonesi, R. Erra-Balsells, J. Heterocycl. Chem. 39 (2002) 933–941.

829 [79] J.Y. Lee, K.W. Song, H.J. Song, D.K. Moon, Synth. Met. 161 (2011) 2434–2440.

830 [80] T. Wang, Z. Zhang, N.A. Meanwell, J.F. Kadow, Z. Yin, Q.M. Xue, A. Regueiro-Ren, J.D.
831 Matiskella, Y. Ueda, US. Pat. Appl. Publ. (2004) US 20040110785.

832 [81] D. Kim, J.K. Lee, S.O. Kang, J. Ko, Tetrahedron 63 (2007) 1913–1922.

833 [82] R. Parthasarathy, B. Paul, W. Korytnyk, J. Am. Chem. Soc. 98 (1976) 6634–6643.

834 [83] T. Murai, F. Hori, T. Maruyama, Org. Lett. 13 (2011) 1718–1721.

835 [84] Z.-C. Song, G.-Y. Ma, H.-L. Zhu, RSC Adv. 5 (2015) 24824–24833.

836 [85] A.R. Stefankiewicz, A. de Cian, J. Harrowfield, CrystEngComm 13 (2011) 7207–7211.

837 [86] Z.-C. Song, G.-Y. Ma, P.-C. Lv, H.-Q. Li, Z.-P. Xiao, H.-L. Zhu, Eur. J. Med. Chem. 44 (2009)
838 3903–3908.

839 [87] A. Bondi, J. Phys. Chem. 68 (1964) 441–451.

840 [88] G.R. Desiraju, T. Steiner, The weak hydrogen bond in structural chemistry and biology, IUCR
841 Monographs on Crystallography, vol. 9, Oxford University Press, Oxford, UK, 1999.

842 [89] J. Gu, W.-Q. Chen, T. Wada, D. Hashizume, X.-M. Duan, CrystEngComm 9 (2007) 541–544.

843 [90] P. Xue, B. Yao, J. Sun, Z. Zhang, R. Lu, Chem. Commun. 50 (2014) 10284–10286.

844 [91] N.A. Kazin, Y.A. Kvashnin, R.A. Irgashev, W. Dehaen, G.L. Rusinov, V.N. Charushin,
845 Tetrahedron Lett. 56 (2015) 1865–1869.

846 [92] J.B. Seneclauze, P. Retailleau, R. Ziessel, New J. Chem. 31 (2007) 1412–1416.

847 [93] Cambridge Crystallographic Data Centre, Available online:
848   www.ccdc.cam.ac.uk/data_request/cif.

849 [94] Y.-W. Li, G.-B. Gu, H.-Y. Liu, H.H.Y. Sung, I.D. Williams, C.-K. Chang, Molecules 10 (2005)
850   912–921.

851 [95] F. Accadbled, B. Tinant, E. Henon, D. Carrez, A. Croisy, S. Bouquillon, Dalton Trans. 39
852   (2010) 8982–8993.

853 [96] C. López, A. Caubet, S. Pérez, X. Solans, M. Font-Bardía, Chem. Commun. (2004) 540–541.

854 [97] C. López, A. Caubet, S. Pérez, X. Solans, M. Font-Bardía, E. Molins, Eur. J. Inorg. Chem.
855   (2006) 3974–3984.

856 [98] D. Talancón, C. López, M. Font-Bardía, T. Calvet, J. Quirante, C. Calvis, R. Messeguer, R.
857   Cortés, M. Cascante, L. Baldomà, J. Badía, J. Inorg. Biochem. 118 (2013) 1–12.

858 [99] M. Crespo, M. Font-Bardía, J. Granell, M. Martínez, X. Solans, Dalton Trans. (2003) 3763–
859   3769.

860 [100] M. Crespo, R. Martín, T. Calvet, M. Font-Bardía, X. Solans, Polyhedron 27 (2008) 2603–2611.

861 [101] C. López, R. Bosque, M. Pujol, J. Simó, E. Sevilla, M. Font-Bardía, R. Messeguer, C. Calvis,
862   Inorganics 2 (2014) 620–648.

863 [102] C. López, C. Moya, P.K. Basu, A. González, X. Solans, M. Font-Bardía, T. Calvet, E. Lalinde,
864   M.T. Moreno, J. Mol. Struct. 999 (2011) 49–59.

865 [103] F.H. Allen, Acta Crystallogr. Sect. B: Struct. Sci. B58 (2002) 380–388.

866 [104] G.A. Crosby, J.N. Demas, J. Phys. Chem. 75 (1971) 991–1024.

867 [105] S. Chattoraj, A. Amin, B. Jana, S. Mohapatra, S. Ghosh, K. Bhattacharyya, ChemPhysChem 17
868   (2016) 253–259.

869 [106] M. Zahedifard, F.L. Faraj, M. Paydar, C.Y. Looi, M. Hajrezaei, M. Hasanpourghadi, B.
870   Kamalidehghan, N.A. Majid, H.M. Ali, M.A. Abdulla, Sci. Rep. 5 (2015) 11544.

871 [107] P.D. Leeson, B. Springthorpe, Nat. Rev. Drug Discov. 6 (2007) 881–890.

872 [108] C.H. Reynolds, B.A. Tounge, S.D. Bembenek, J. Med. Chem. 51 (2008) 2432–2438.

873 [109] J.A. Arnott, R. Kumar, S.L. Planey, J. Appl. Biopharm. Pharmacokinet. 1 (2013) 31–36.

874   [110]   K.D. Freeman-Cook, R.L. Hoffman, T.W. Johnson, Future Med. Chem. 5 (2013) 113–115.

875   [111]   W. Wang, X. Sun, D. Sun, S. Li, Y. Yu, T. Yang, J. Yao, Z. Chen, L. Duan, ChemMedChem 11
876   (2016) 2675–2681.

877   [112]   For a general overview of the role of Topoisomerases in cancer see for instance: Y. Xu, C. Her,
878   Biomolecules 5 (2015) 1652–1670.

879   [113]   S.P. Fricker, Metallomics 2 (2010) 366–377.

880

881 **Legends to figures**

882

883 **Figure. 1**. Carbazole and two naturally occurring carbazole derivatives (Ellipticine and Glybomine-B

884 and C) with potent cytotoxic activities in front of several cancer cell lines.

885

886 **Scheme 1** Synthesis of carbazoles 1a and 1b. Reagents and conditions: i) KI, KIO3, acetic acid, reflux.

887 ii) NaH, DMF, room temperature followed by treatment with iodomethane, in DMF at room

888 temperature. iii) 2-(Tributylstannyl) thiazole, [Pd(PPh3)4], DMF, 100 °C. iv) 2-

889 (Tributylstannyl)thiophene, [Pd (PPh3)4], DMF, 100 °C.

890

891 **Figure. 2**. Atom labelling scheme for ligands 1a and 1b.

892

893 **Figure. 3**.Molecular structure and atom labelling scheme for the new hybrid carbazole-thiazole ligand

894 (1a).

895

896 **Figure. 4** Schematic view of: A) the assembly of a molecule of 1a, sited at (x, y, z) and another unit at

897 (−1+x, y, z) by π-π stacking between the thiazolyl and the phenyl ring of the carbazole (in purple) and

898 CeH···π short contacts (green dotted lines) involving one of the methyl protons (H10) and the

899 propagation of these interactions along the crystal to give pillars; B) simplified view of connectivity of

900 the pillars through CeH···π contacts.

901

902 **Scheme 2** Synthesis of the complexes. Reagents and conditions: i) trans-[PdCl2(dmso)2] in refluxing

903 methanol (1 h) or Na2[PdCl4] in methanol at 298 K, 24 h [molar ratios Pd(II):1a=1:1 and 1:2,

904 respectively]; ii) cis-[PtCl2(dmso)2] in refluxing methanol (1 h) and iii) equimolar amounts of cis-

905 [PtCl2(dmso)2] and NaOAc in a toluene: MeOH (5:1) mixture under reflux {see text and Table 2,

906 (entries V and VI)}.

907

908 **Figure. 5**..Highest occupied molecular orbital (HOMO) and lowest unoccupied molecular orbital

909 (LUMO) for the new carbazole derivatives (1a and 1b).

910

911 **Figure. 6**..Plot of the energy of the molecule of 1a (blue) or 1b (red) versus the value of the torsion

912 angle S1-C2'-C3-C4 (φ). (For interpretation of the references to colour in this figure legend, the reader

913 is referred to the web version of this article.)

914

Figure. 7. Comparative plot of the IC50 values (in μM) of the new carbazoles (1a and 1b), the Pd(II) and Pt(II) complexes derived from 1a and cisplatin in front of the colon cancer cell line (HCT116) and the two breast cancer cell lines (MDA-MB231 and MCF7).

Figure. 8. Interaction of pBluescript SK+ plasmid DNA (40 μg/mL) with increasing concentrations of compounds 1a, 1b, 2a and 3a, ethidium bromide (EB) and cisplatin. Lane 1: DNA only; Lane 2: 1 μM; Lane 3: 2.5 μM; Lane 4: 5 μM; Lane 5: 10 μM; Lane 6: 25 μM; Lane 7: 50 μM; Lane 8: 100 μM; Lane 9: 200 μM. Ccc represents the supercoiled closed circular form and oc the open circular form.

Figure 9.Analysis of the new ligands (1a and 1b) and compounds 2a and 3a as potential DNA intercalators or Topoisomerase I inhibitors. Conversion of supercoiled pBluescript SK+ DNA (40 μg/mL) to relaxed DNA by the action of Topoisomerase I (3 units) in the absence or in the presence of increasing amounts of compounds. E=100 μM etoposide; EB=10 μM Ethidium Bromide; SC=supercoiled DNA as control; R=relaxed DNA by the action of Topoisomerase I as control; Lane 1: 100 μM; Lane 2: 200 μM; ccc=closed circular form and oc=open circular form.

Figure. 10. A) Topoisomerase-II α inhibitory activity of compounds 1a, 1b, 2a and 3a. Reactions contained supercoiled plasmid DNA, Topoisomerase IIα (4 units) and 100 μM of the indicated compound. B) Topoisomerase IIα inhibitory activity of compound 2a at different concentrations: Lane 1: 50 μM; Lane 2: 100 μM and Lane 3: 200 μM. In all experiments, control reactions were performed in the presence of: E: etoposide at 100 μM; P: SC Plasmid DNA only; T: reaction performed with plasmid DNA and Topoisomerase IIα (4 units).
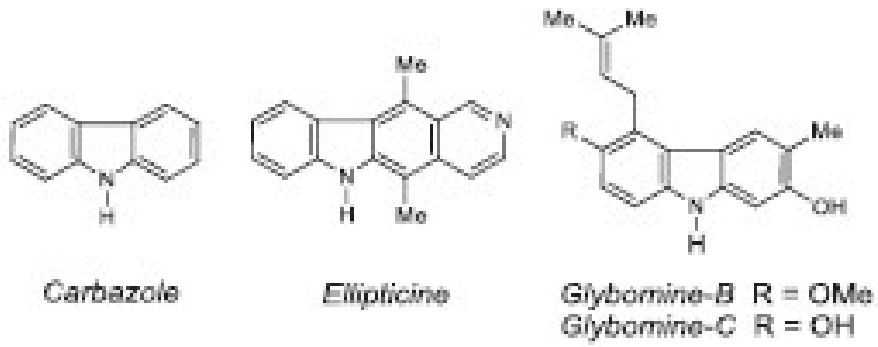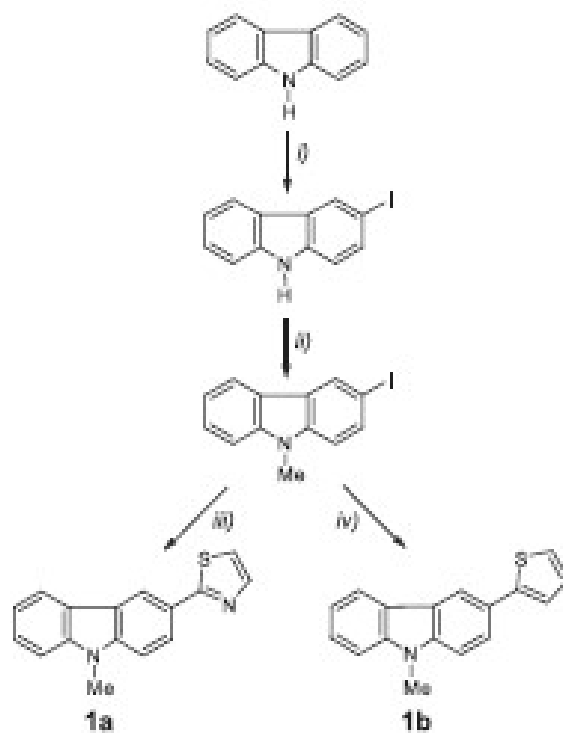
FIGURE 1

Carbazole

Ellipticine

Glybomine-B R = OMe
Glybomine-C R = OH

SCHEME 1

FIGURE 2

1a   1b

FIGURE 3

FIGURE 4

SCHEME 2

FIGURE 5

968
969
970

971
972

FIGURE 6

FIGURE 7

FIGURE 8

FIGURE 9

991

FIGURE 10

992

993
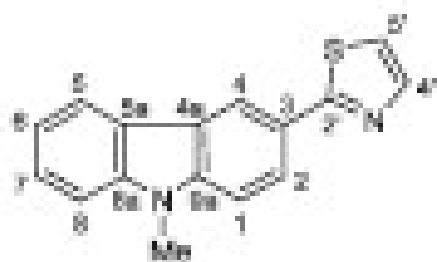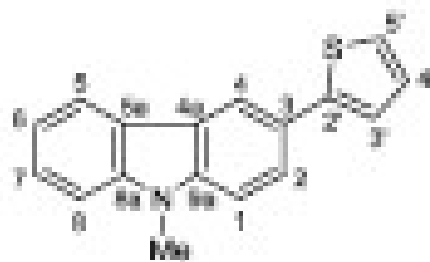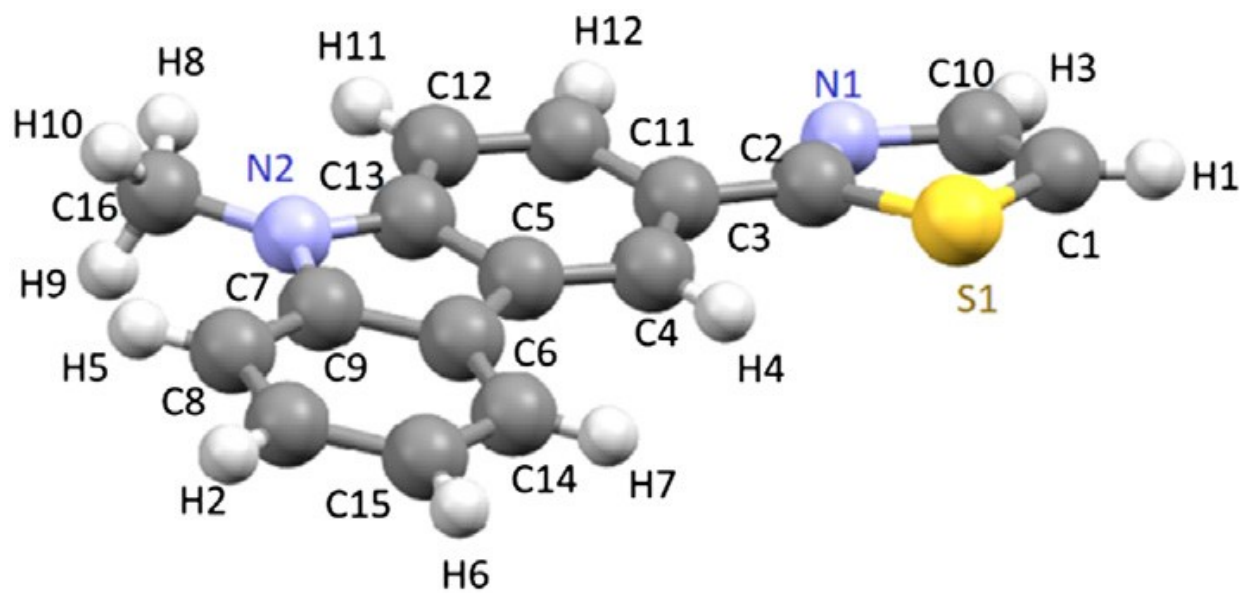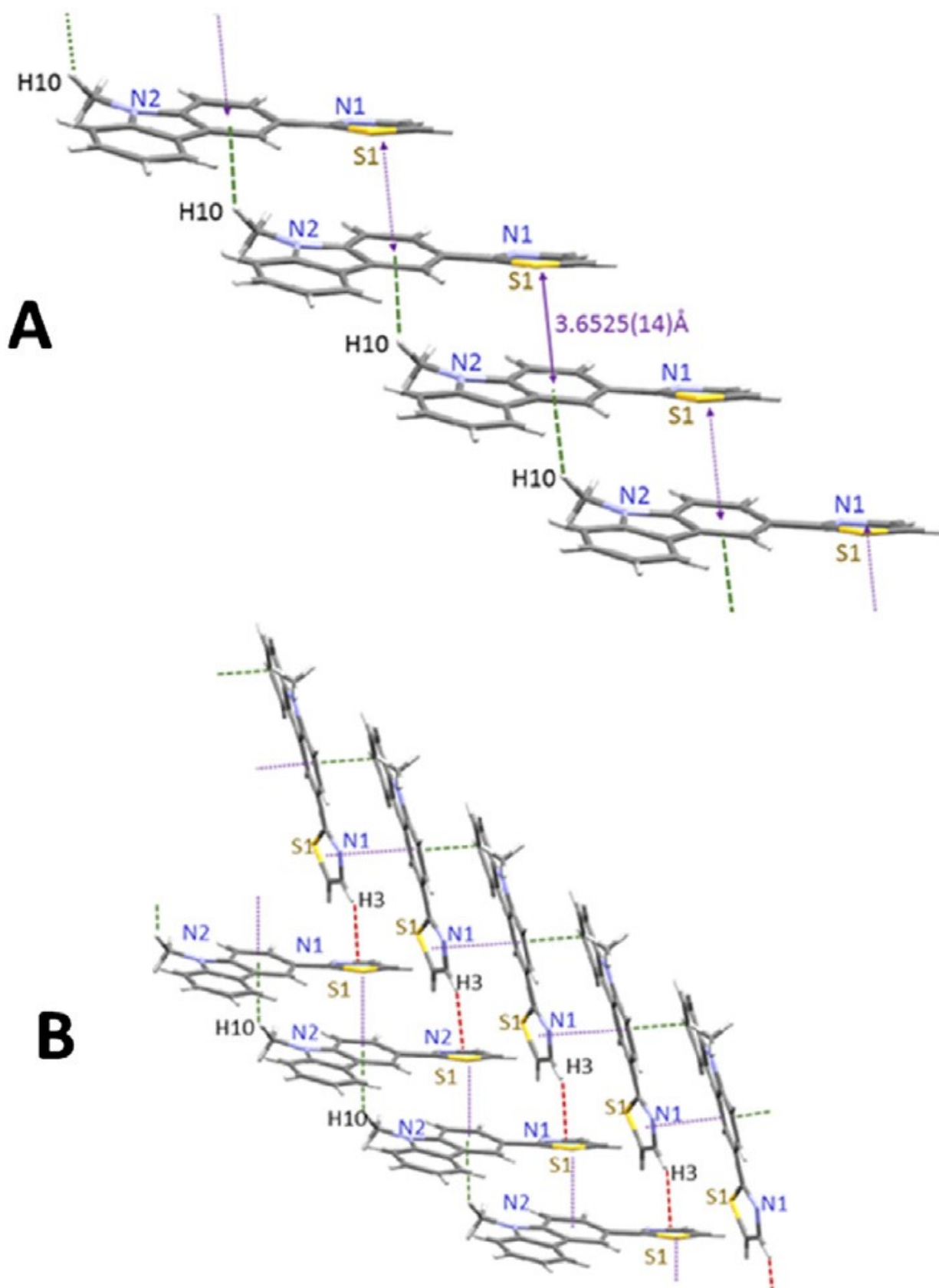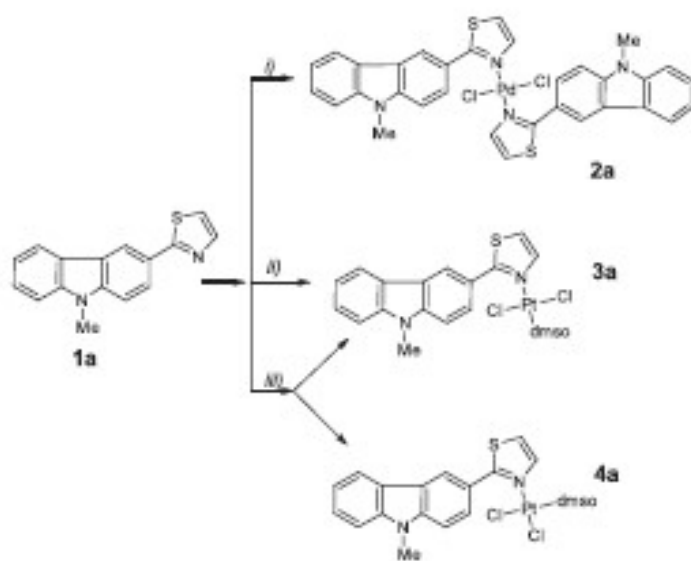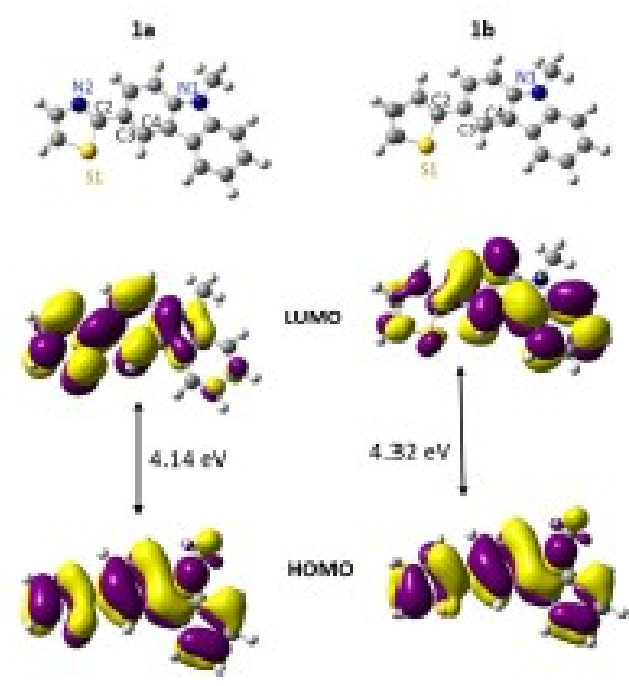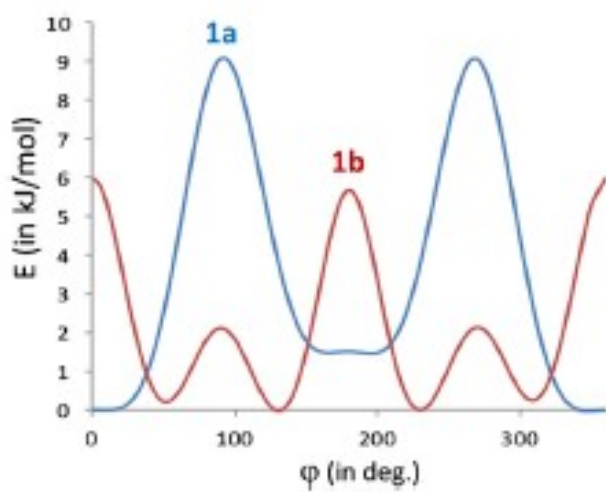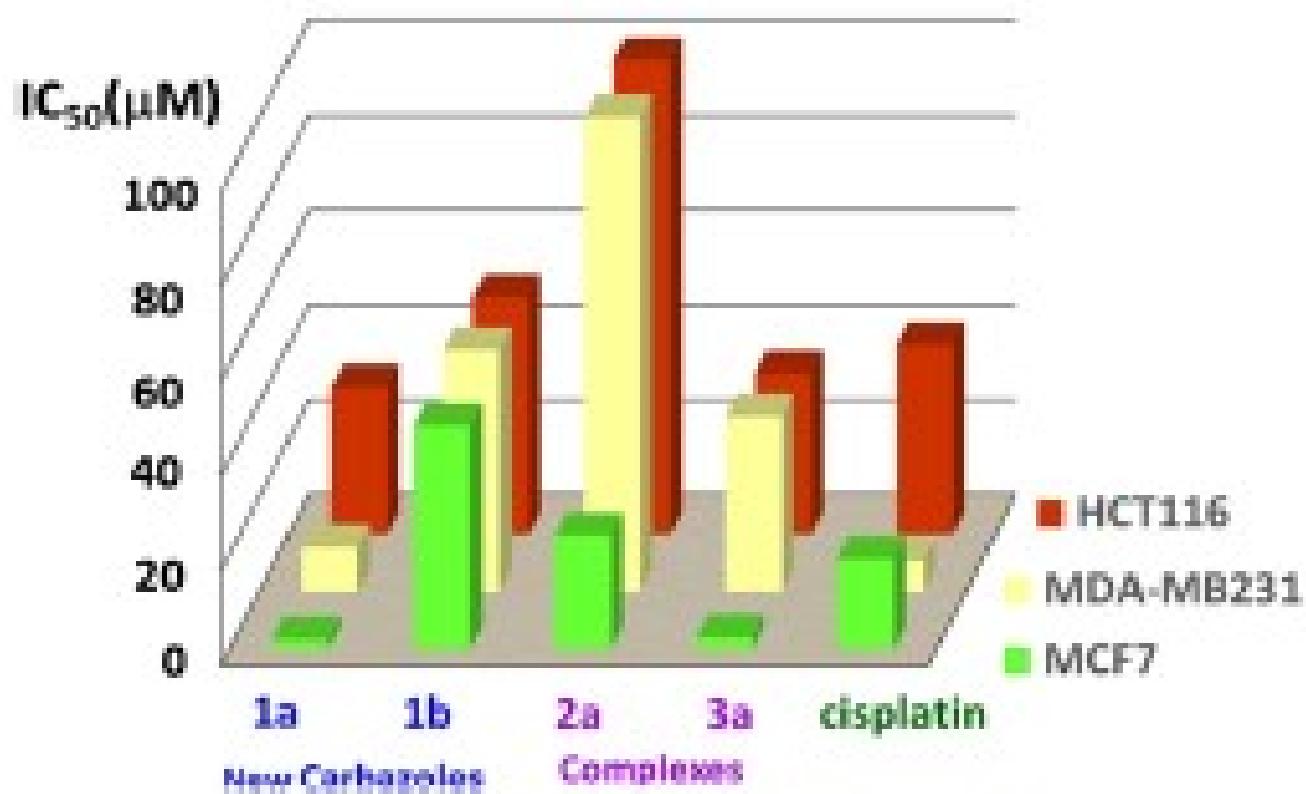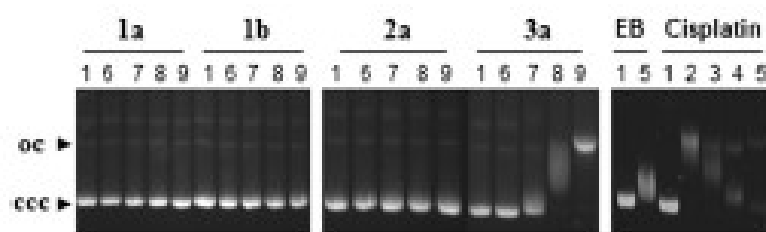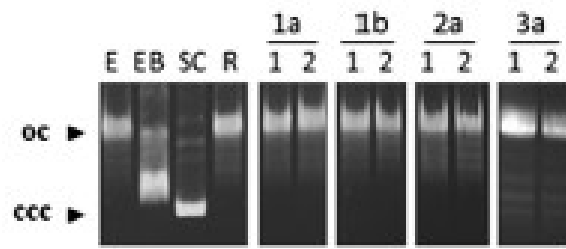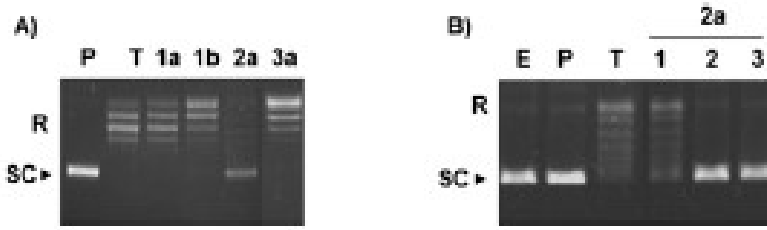
994

995 **Table 1**.. Crystal data and details of the refinement for compound 1a.

996

Empirical formula	$C_{16}H_{12}N_2S$
Formula weight	264.34
Temperature/K	100(2)
λ/Å	0.71073
Crystal sizes/mm × mm × mm	0.292 × 0.168 × 0.048
Crystal system	Orthorhombic
Space group	$P2_12_12_1$
a/Å	6.0702(2)
b/Å	12.8577(5)
c/Å	16.0721(6)
$\alpha = \beta = \gamma$/deg.	90
V/Å^3	1254.41(8)
Z	4
Density (calculated) /Mg × m^{-3}	1.400
μ/mm^{-1}	0.243
F(000)	552
Θ range for data collection/deg.	from 2.028 to 27.498
Index ranges	$-7 \le h \le 7, -16 \le k \le 16, -20 \le l \le 20$
Completeness to $\Theta = 25.242°$	99.9%
Absorption correction	Semi-empirical from equivalents
Max. and min. transmission	0.7456 and 0.6711
Refinement method	Full-matrix least-squares on F^2
Data/restraints / parameters	2855/0/173
Goodness-of-fit on F^2	1.074
Final R indices [$I > 2\sigma(I)$]	$R_1 = 0.0358, wR_2 = 0.0743$
R indices (all data)	$R_1 = 0.0471, wR_2 = 0.0801$
Absolute structure parameter	0.04(4)
Largest diff. peak and hole/e.Å^{-3}	0.341 and −0.234

997
998

999 **Table 2** Summary of experimental conditions [reagents, molar ratios (1a:Pd(II) or 1a:Pt(II)), solvents,

1000 temperature (T), reaction time (t, in h)] used in the study of the reactivity of carbazole 1a with trans-

1001 [PdCl2(dmso)2], Na2[PdCl4] or cis-[PtCl2(dmso)2].

1002

Entry	Reagents	Molar ratios	Solvent	T	t	Final products
I	1a: trans-[PdCl₂(dmso)₂]	(1:1) or (2:1)	MeOH	Reflux	1	2a
II	1a: Na₂[PdCl₄]	(1:1) or (2:1)	MeOH	298 K	24	2a
III	1a: cis-[PtCl₂(dmso)₂]	(1:1)	MeOH	Reflux	1	3a
IV	1a: cis-[PtCl₂(dmso)₂]	(1:1)	MeOH	Reflux	24	3a
V	1a: cis-[PtCl₂(dmso)₂]: NaOAc	(1:1:1)	Toluene/MeOH[a]	Reflux	24	3a and 4a[b]
VI	1a: cis-[PtCl₂(dmso)₂]: NaOAc	(1:1:1)	Toluene/MeOH[a]	Reflux	72	3a and 4a[c]

[a] A 5:1 mixture.
[b] Only traces of compound 4a were detected.
1003 [c] Integration of the signals observed in the ^{1}H-NMR spectrum of the raw material indicated that the molar ratio 3a:4a was 1.7.

1004

1005 **Table 3** Absorption and emission properties of the free carbazoles (1a and 1b) and the Pd(II) and Pt(II)

1006 complexes (2a and 3a, respectively) in CH2Cl2 [Wavelengths λi (in nm), logarithms of the extinction

1007 coefficients (log εi), emission wavelengths [λem (in nm) after excitation at λexc=300 nm] and quantum

1008 yields (Φ).

1009

Compd.	Absorption spectroscopic data	Emission spectroscopic data	
	λ (log ε)	λ_{em}	Φ
1a	328 (4.3), 301 (4.5), 279 sh (=4.2)	370 sh, 384	0.22
1b	317 (=4.2), 299 (4.5)	376, 394	0.12
2a	334 (3.6), 300 (3.8), 284 (=3.8)	370 sh, 385	0.02
3a	346 (4.2), 301 (4.4), 287 (4.4)	370 sh, 386	< 0.01

1010
1011
1012
1013
1014

1015 **Table 4** Cytotoxic activities (IC50 valuesa, µM) on the cancer cell lines: HCT116 (colon), MDA-

1016 MB231 and MCF7 (breast) and the normal non-tumoral human skin fibroblast BJ cells, for 1a, 1b and

1017 the palladium(II) and platinum(II) complexes derived from 1a (2a and 3a, respectively) and for cisplatin.

1018 For comparison purposes, Clog P valuesb and lipophilic efficiencies (LipEc) of compounds 1a, 1b, 2a

1019 and 3a on the MCF7 cell line are also included

1020

Compounds	IC_{50} values in the cell lines[a]				ClogP[b]	LipE[c]
	HCT116	MDA-MB231	MCF7	BJ		
Carbazoles						
1a	31 ± 2	9.4 ± 2.6	2.0 ± 0.5	> 100	4.42	1.27
1b	50 ± 4	51 ± 3	47 ± 3	> 100	5.73	−1.39
Complexes						
2a	> 100	> 100	24 ± 2	> 100	9.42	−4.80
3a	34 ± 3.5	37 ± 3.6	2.4 ± 2.2	> 100	4.33	1.29
Cisplatin	40 ± 4.4	6.5 ± 2.4	19 ± 4.5	12 ± 2	–	–

[a] Data are shown as the mean values of two experiments performed in triplicate.

[b] ClogP is the calculated logarithmic value of the n-octanol/water partition coefficient and was calculated using the ChemBioDrawUltra computer program.

[c] LipE indexes were calculated as $LipE = -\log(IC_{50}) - ClogP$ [107–110] and using the IC_{50} values obtained in the MCF7 cell line.

1021
1022
1023
1024